ABSTRACT

The objective of this work was to fabricate gelatin and alpha-tricalcium phosphate (α-TCP) scaffolds via freeze-drying technique. Both materials are well known to be promising candidates for tissue engineering and drug delivery applications. One of the main characteristics that we look for in scaffolds and drug delivery systems is the formation of an adequate porosity. The role of this porosity is to ensure cell colonisation, flow transport of nutrients and metabolic waste in scaffolds for tissue engineering and to enhance the loading capacity and delivery rate in delivery systems.

Two types of scaffolds were produced: one of organic matrix reinforced by an inorganic phase (α-TCP) and the other of inorganic matrix (α-TCP) with gelatin as a binder. Organic phase plays an important role in the toughness of bone whereas inorganic phase enhances its mechanical properties.

The aim was to produce scaffolds with organic matrix and enhance the existing process, and also create new scaffolds with inorganic matrix. Different strategies were tested in order to optimize the fabrication process of the scaffolds.

Characterization of the scaffolds included: microstructural evaluation by scanning electron microscopy, evaluation of the percentage of isolated porosity by helium pycnometry, rigidity test by mechanical testing and the study of the proportion of phases in the scaffold by X-ray diffraction analysis.

The structure network has been improved in the case of scaffolds with organic matrix, by decreasing the content of closed pores and also by ensuring total incorporation of the α-TCP powder in the scaffold. Regarding the creation of scaffolds of inorganic matrix, the results, in terms of porosity and mechanical properties, were very promising and opened a new area of investigation.

INDEX

1. GLOSSARY

α-TCP : α phase of tricalcium phosphate, α-$Ca_3(PO_4)_2$.

β-TCP : β phase of tricalcium phosphate, β- $Ca_3(PO_4)_2$.

Bioactivity: ability to create a bond with the bone, without interposition of a fibril capsule.

Biocompatibility: quality of not having toxic or injurious effects on biological systems

CDHA: Calcium deficient hydroxyapatite $Ca_9(HPO_4)$ $(PO_4)_5OH$. It is obtained by the dissolution and precipitation of the alpha tricalcium phosphate.

HA: hydroxyapatite, $Ca_{10}(PO_4)_6(OH)_2$

Macroporosity: pores greater than 50 nm

Microporosity: pores with diameters of less than 2 nm

PHA: precipitated hydroxyapatite

Porosity: The ratio of the volume of closed pores and connected pores in a material to the volume of the whole.

SEM: Scanning Electron Microscopy

Tissue engineering: field that applies the principles of engineering and life science for the development of biological substitute that restore, maintain or improve tissue or organ function.

2. INTRODUCTION

The present project takes place in the field of tissue engineering. One of the branches in tissue engineering explores the possibility of creating scaffolds with an adequate porosity in order to favor cells invasion and enhance bone regeneration.

Not only the porosity has to be adequate, the choice of the materials used to fabricate these scaffolds is also another important criterion. Gelatin is a derivate of collagen, which is the main organic phase of the bone and α-TCP hydrolizes into calcium deficient hydroxyapatite, the inorganic phase of the bone.

The principal aim of this work is the development of scaffolds made of gelatin and α-TCP for tissue regeneration. Two different families of scaffolds of either organic or inorganic matrix have been studied in order to provide samples with a wide variety of mechanical and chemical properties.

These specific materials must be highly porous (with pores superior to 100μm), with an interconnected pore network to assure cells circulation.

This work contains the enhancement of a fabrication process of scaffolds with organic matrix, but especially the creation of scaffolds with inorganic matrix.

These scaffolds have a macroporosity induced by freeze drying. This technique was prefered among others which required the use of toxic solvents.

3. STATE OF ART

3.1 Composition of bones

Bones are rigid body tissue consisting of cells embedded in an abundant, hard extra cellular matrix. Its structure can be observed in the figure 3.1. The two principal components of this material are collagen and tri-calcium phosphate, which stand for respectively the organic phase and the inorganic phase.

- Collagen is a long and fibrous structural protein. It consists of amino acid sequences that coil into a triple helical structure to form very strong fibers. Because of this special structure, it renders elasticity and flexibility to the bone. Collagen is 36% of the total bone volume.

- Calcium phosphate, and especially hydroxyapatite, is the mineral structure of the bone. The aim of this phase is to give a significant rigidity to the bone. This inorganic phase is 64% of the total bone volume.

The combination of those two phases, organic and inorganic, make bones relatively light weighted, strong and hard, making them the best candidate for the protection of internal organs such as the skull protecting the brain or the ribs protecting the heart and lungs. They also have a metabolic function, being the principal reserve of calcium in the body, and overall a mechanical function, they are the support of the tissues and the point of attachment of the muscles: they provide our locomotion. (1)

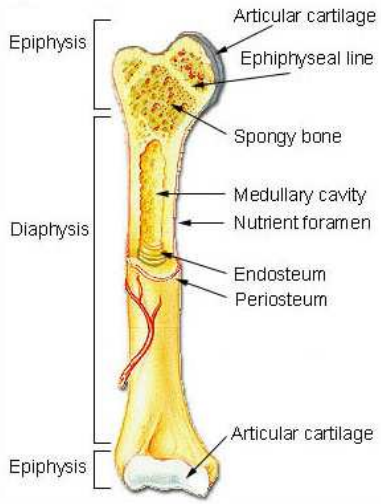

Fig 3.1: Bone structure (2)

3.2 Spongy bone and cortical bone

There are two types of bone tissue: compact and spongy. In the following figure 3.2, a bone is presented and these two parts are clearly illustrated.

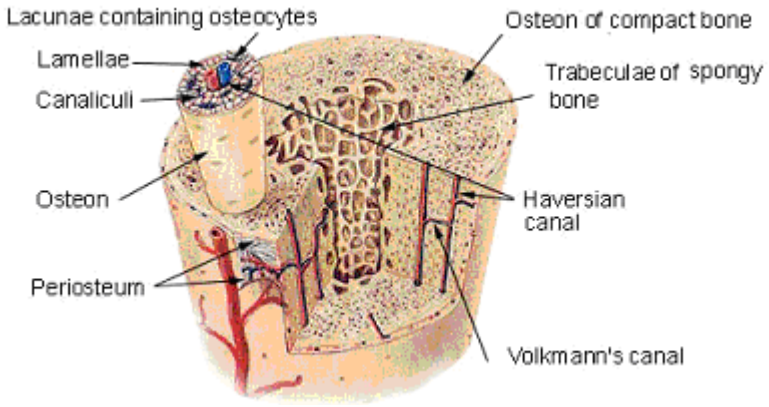

Fig 3.2: Compact bone and spongy bone (2)

Compact bone, also called cortical bone, forms the surface of all bones. It is dense and forms the surface of bones, contributing 80% of the weight of a human skeleton. The bony matrix is solidly filled with organic ground substance and inorganic salts, leaving only tiny spaces (lacunae) that contain the osteocytes, or bone cells. It is extremely hard, its young modulus is around 18Mpa. (1)

Spongy bone is the tissue that makes up the interior of bones. It is a connected network of rods or plates. Its structure is an open cell porous network, and this type of bone is also called cancellous bone. It has less density than the compact bone.

3.3 The inorganic phase: the hydroxyapatite-like phase

Hydroxyapatite-like phase is the component of the mineral phase in bones, while hydroxyapatite, HA, has a specific chemical composition $Ca_{10}(PO_4)_6$ $(OH)_2$. Bone is best described as a calcium deficient hydroxyapatite, CDHA, $Ca_9(HPO_4)$ $(PO_4)_5OH$. (1)

This material is bioactive. Bioactivity is the characteristics of an implant material which allows it to form a bond with living tissues and so that to have a very good integration in the human body.

Hydroxyapatite forms part of the crystallographic family of apatites, isomorphic compounds with the same hexagonal structure. Hydroxyapatite can crystallize to form plates or needles. They are deposited parallel to the collagen fibres, such that the larger dimension of crystals is along the long axis of the fibre.

The chemical nature of hydroxyapatite lends itself to substitution: the most common substitutions involve carbonate, phosphate, magnesium substitutions for hydroxyl groups. (1)

3.4 The organic phase: the collagen

Collagen is the main protein of connective tissue in animals and the most abundant protein in mammals.

The collagen molecule is made up of three polypeptide strands (called alpha peptides), each possessing the conformation of a helix. These three helices are twisted together into a triple helix. It has great tensile strength, and is the main component of ligaments and tendons. It is responsible for skin elasticity, and its degradation leads to wrinkles that accompany aging. (1)

Type I collagen fibrils have enormous tensile strength; that is, such collagen can be stretched without being broken. These fibrils, roughly 50 nm in diameter and several micrometers long, are packed side-by-side in parallel bundles, called collagen fibres, in tendons, where they connect muscles with bones and must withstand enormous forces

After reducing crosslinkages between collagen components and removing some of

the impurities such as fat and salts, partially purified collagen is converted into gelatin by extraction with either water or acid solutions at appropriate temperatures. This extraction is one of the most important step in gelatin production. (1)

3.5 The gelatin

Gelatin is the derived protein that can be obtained as a breakdown product of collagen by extracting collagen-source materials with hot water above 40ºC.

The method of preparation is the following:

i) the raw material is pretreated with either acid or alkaline solution

ii) gelatin is then fractionally extracted by heating process at increasing temperatures

iii) the resulting bouillon is treated by some classic techniques such as settling, filtration, centrifugation... to obtain the final product.

The acid-extracted gelatin is designated "Type A", whereas the product of the alkaline method is referred to as "Type B".

Gelatin, under its liquid form, is capable of forming and stabilizing hydrogen bonds with water molecules to form a stable three-dimensional gel. For specific biological applications, this transformation, called gelation, is necessary. It is basically induced by the formation of a three-dimensional network. The gel point is considered as the point at which the viscosity begins to increase abruptly with decreasing temperature. (3)

By cooling the solution, the formation of single helices from the random coils of gelatin chains begins. Each gelatin chain has several random coil segments along the chain. As the solution is further cooled, triple helix formation starts, a process which continues down to temperatures below the melting point. The properties of gelatin gels are intimately dependent on the speed of cooling the gelatin sols and the degree of acidity. Slow cooling would permit better orientation of gelatin molecules for gel formation. It cooled to reach the consistency of thick egg white.

3.6 Crosslinking process

This process makes the gelatin resistant to dissolution in water. These reactions result in structural modifications that can increase the rigidity of gelatin. (7)

EDC (acronym for 1-ethyl-3-(3-dimethylaminopropyl) carbodiimide hydrochloride)) is a water soluble carbodiimide. It is generally used for protein crosslinking to nucleic acids. EDC is often used in combination with N-hydroxysuccinimide (NHS) or sulfo-NHS to increase coupling efficiency or create a stable amine-reactive product. Molecules like NHS can also react with carboxylic groups in order to increase the amount of crosslinks.

The formula of the complete molecule is also given below in the figure 3.6.

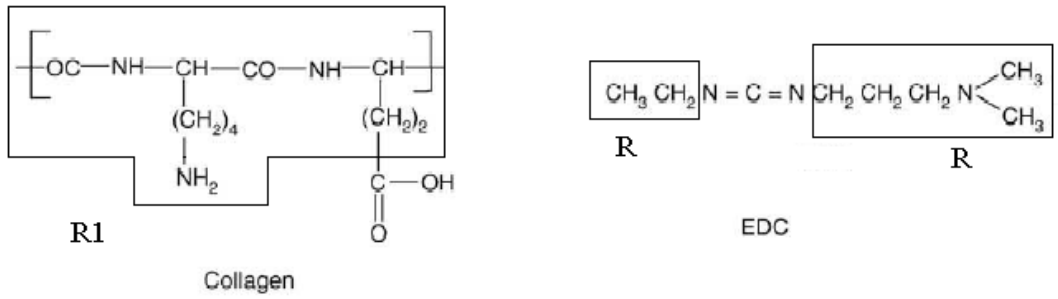

Fig 3.6: molecule of collagen and EDC

The mechanism of reaction with the carboxylic acids is presented in the figure 3.7.

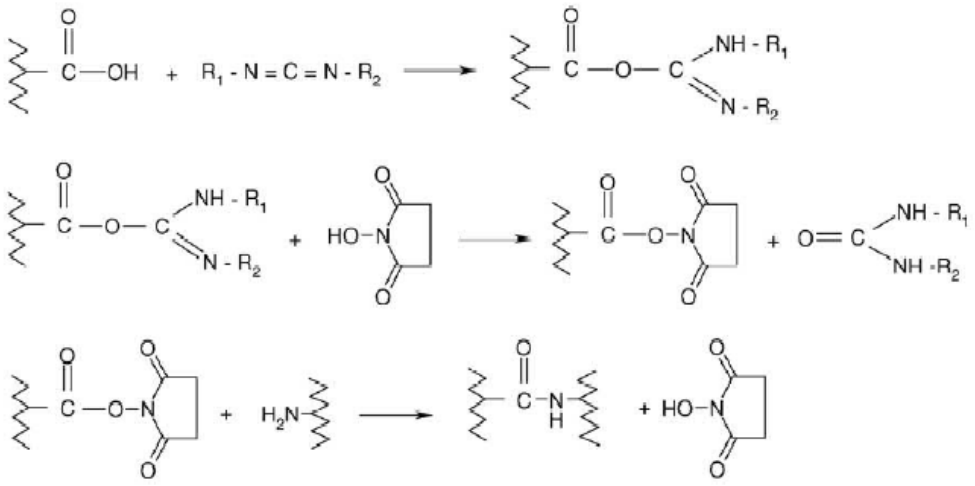

Figure 3.7: Mechanism of the reaction

3.7 Calcium phosphate cements

Generally speaking, calcium phosphate cements are obtained by mixing one or several reactive calcium phosphate powders with an aqueous solution to form a paste. Then, the cement sets, following a process of dissolution and precipitation. (4)

The mixture transforms into HA during setting, forming a porous body even at 37ºC. The setting time of calcium phosphate cements can be decreased even to a few minutes.

Easy shaping of the calcium phosphate bone cements enables using them to fill the bone defects much better than the HA solid blocks, which are difficult to shape, or the HAp powders/granules, which are difficult to keep in place. (5)

Indeed, this type of material offers a large range of possibility like the surgeon moldability, injectability, complete filling of an empty cavity…it has also the huge advantage of an acceptable clinical time, which means that the duration between the moment of injection of the paste and hardening of the cement is coherent for a surgery application. (5)

Some important conditions in the area of bone tissue engineering have to be followed, for in-vivo but also in-vitro experiments. Biocompatibility, controlled degradation, osteoconductivity, formability are a few of them.

It exists several solid phases which can lead to a calcium phosphate cement.

Compound	Formula	Ca/P ratio
α-TCP, α-Tricalcium phosphate	α-$Ca_3(PO_4)_2$	1.5
β-TCP, β-Tricalcium phosphate	β- $Ca_3(PO_4)_2$	1.5
OCP, Octacalcium phosphate	$Ca_8H_2(PO_4)_6.5H_2O$	1.33
HA, Hydroxyapatite	$Ca_5(PO_4)_3(OH)$	1.67
TTCP, Tetracalcium phosphate	$Ca_4(PO_4)_2O$	2.0
DCP, Dicalcium phosphate	$CaHPO_4$	1
MCPM, Monocalcium phosphate monohydrate	$Ca(H_2PO_4)_2.H_2O$	0.5
MCPA, Monocalcium phosphate anhydrous	$Ca(H_2PO_4)_2$	0.5
DCPD, Dicalcium phosphate dihydrate	$CaHPO_4.2H_2O$	1
PHA, Precipitated hydroxyapatite	$Ca_{10}(PO_4)_6(OH)_2$	1.67
CDHA, Calcium deficient hydroxyapatite	$Ca_9(HPO_4)(PO_4)_5OH$	1.5

Fig 3.3: Calcium phosphate prepared by solid state reactions (4)

The figure 3.3 presents a table of all of the principal calcium phosphates which have a biological interest.

The fabrication of a cement (setting time) is divided in 3 parts:

- Dough period: time needed for a well-mixed preparation. Powder and water form a homogeny paste.

- Working period: laps time during operator can work with the paste without modify its structure.

- Curing period: time for the setting operation, when viscosity increases. When it stops increasing, setting is finished.

Setting time cannot be more than 15 minutes, because of the application we would like to do, inject the cement in the body. We can also quote products which can accelerate the reaction, temperature, and the fraction of PHA introduced because its role is to catalyze. (4)

Then, cements are placed into physiological environment, which means at neutral pH and 37ºC and the hardening operation begins.

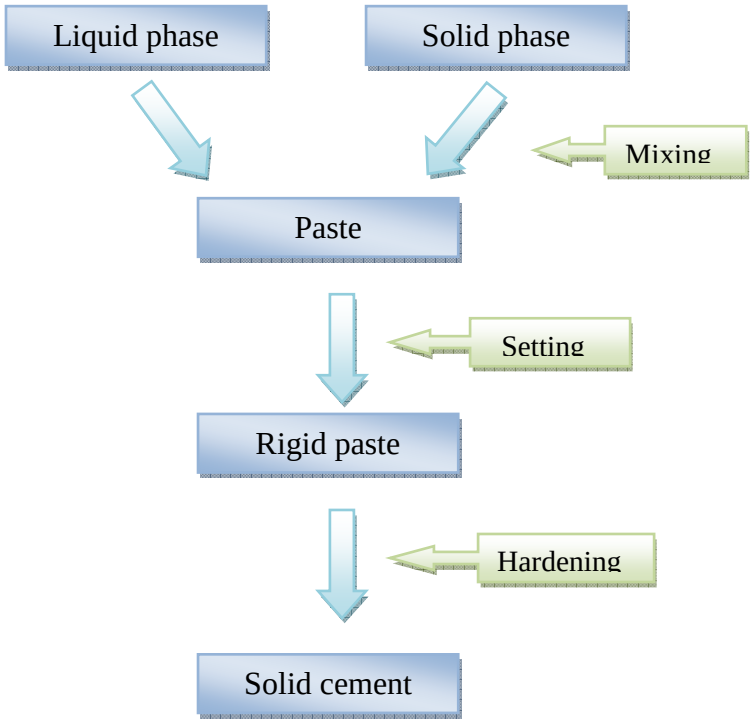

Fig 3.4: Chronology of the fabrication of a cement

During the setting and the hardening time, explained in the figure 3.4, the hydrolysis of the α-TCP leads to the synthesis of the calcium deficient hydroxyapatite. The reaction is the following:

$$3\text{-}\alpha\text{-}Ca_3(PO_4)_2 + H_2O \longrightarrow Ca_9(HPO_4)(PO_4)_5OH$$

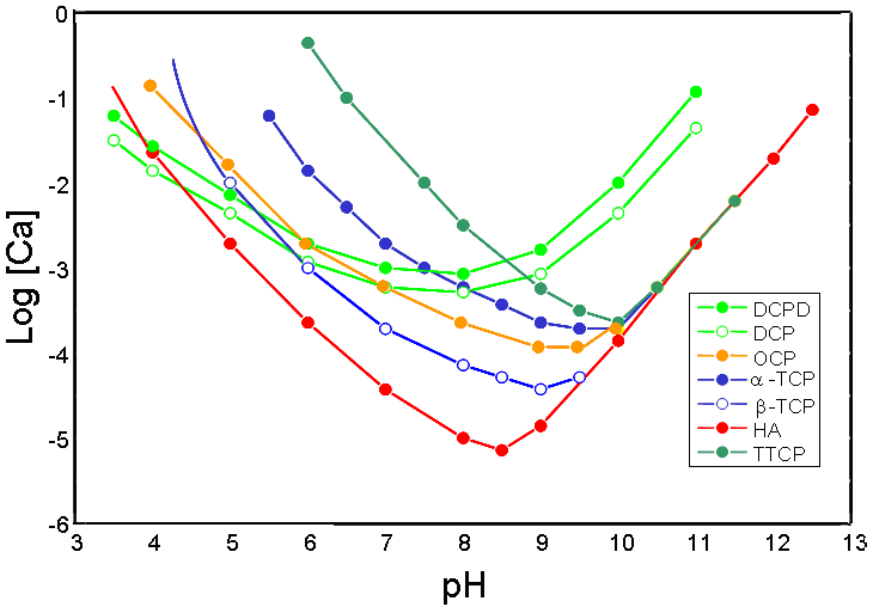

Fig 3.5: Solubility isotherms of different calcium phosphate salts in equilibrium with their solutions for the ternary system $Ca(OH)_2.H_3PO_4.H_2O$ at 37·C in a representation of log [Ca] versus pH (7)

Figure 3.5 demonstrate the relative stability of the different salts at different pH values. They become more soluble as the pH decreases. HA is the least soluble, and so that the more stable at pH neutral. (5) Under the solubility isotherm, there is the undersaturate area, where the solid tends to dissolve to reach the equilibrium. Over the solubility isotherm, the solid tends to precipitate until the equilibrium as well. (6)

Among all solid phases used for the preparation of cements, the best for the specific application of bone regeneration seems to be the alpha-tricalcium phosphate (α-TCP). When α-TCP is dissolved, the liquid phase created around α-TCP particles becomes supersaturated of ions calcium and phosphate. The result is a paste which follows a mechanism of dissolution and precipitation, during setting and hardening operation.

3.8 Tissue engineering

Tissue engineering involves the use of cells to regenerate the damaged tissue. In order to maintain the tissue-specific functions of the cells, once implanted, a substrate material must be inserted to aid in organization of the cells. (7) Tissue engineering is illustrated in the figure 3.8.

To provide a three-dimensional template for tissue growth, a material used as a scaffold must be able to withstand the mechanical loading necessary to facilitate bone growth. This scaffold material must degrade in vivo but must do so at a rate so as not to compromise the mechanical stability of the scaffold prior to sufficient bony ingrowth. (7)

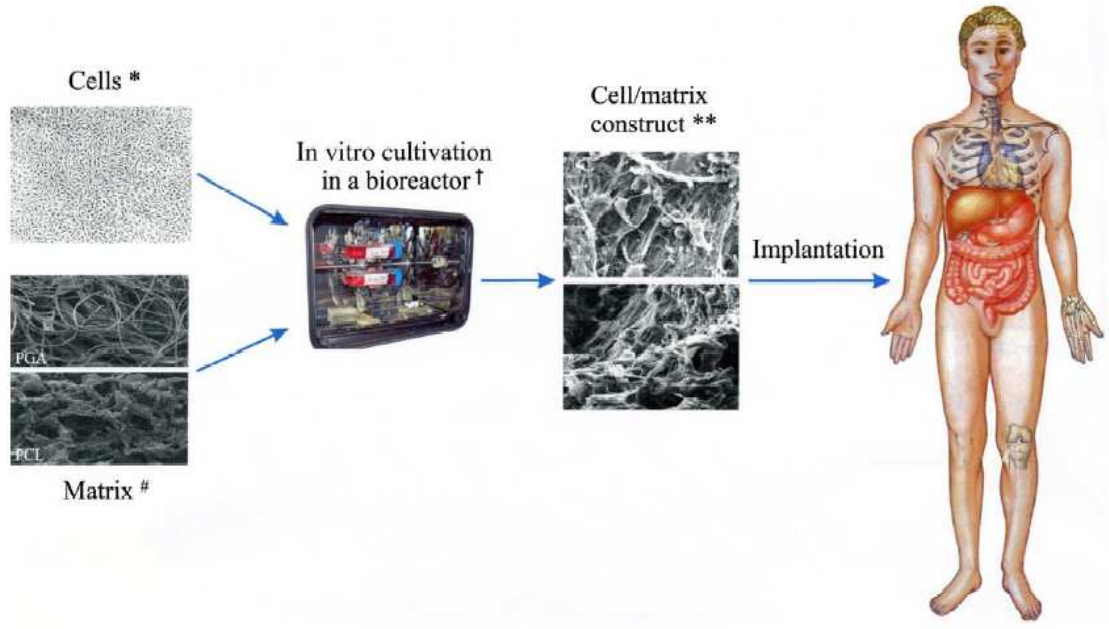

Fig 3.8: Tissue engineering (8)

3.9 The porosity: a crucial point

A crucial point to get all these conditions is porosity. It can act as a reservoir, for cells installation for example, or as a path for transport of proteins…The more the porosity is interconnected, the best is to ensure all that. It also allows the elimination of non-wanting gases.

In reality, intrinsic porosity is created in the cements after their setting and hardening. But this porosity is qualified of nano and microporosity, and it is necessary to add macroporosity above 100µm to allow cell colonisation. It means that cements on their own don't really have an interest here. Another method is needed to create the required porosity, and it is the point of this work.

Pore size is expressed in term of the diameter (or radius) of the opening. Porosity has a classification system as defined by IUPAC (International Union of Pure and Applied Chemistry), which gives a guideline of pore widths applicable to all forms of porosity. (9) The classification is as follows: pores with diameters of less than 2 nanometers are referred as micropores. Those with a diameter from 2nm to 50nm are mesopores. Pores with larger diameter are macropores. (9)

The porosity of the set CPCs is closely related to the liquid/powder ratio used, and it normally varies between 30% and 50%, although even higher values can be reached. The pores are normally micropores or mesopores. However, parameters such as particle size distribution of the starting powder can modify the size of the precipitated crystals, and also the pore size distribution.

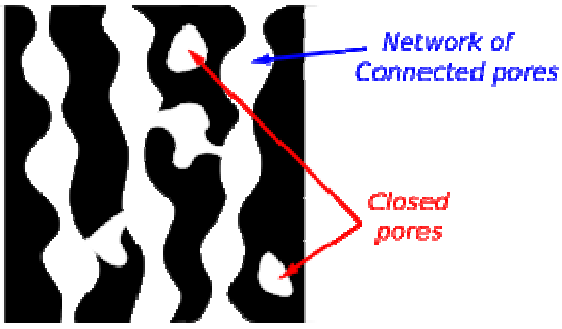

Fig 3.9: Schematic representation of a porous network

Pores which are connected are in contact with the external surface of the sample and allow the passage of an adsorbate through it (figure 3.9).

A closed pore is a void within the scaffold which is not connected to the external surface and hence is isolated (figure 3.9).

3.10 Techniques to create porous scaffolds

The minimum pore size for in vivo bone ingrowth into a material 100 µm; therefore, an ideal scaffold would have interconnects of at least 100 µm in diameter between its macropores. It is therefore really important to be able to quantify both the pores and interconnects to optimise tissue scaffolds. The interconnectivity of the pores also dominates the flow properties, which are important to ensure adequate delivery of cells during seeding and nutrient during subsequent culture. Other criteria include the scaffold material should promote cell adhesion and activity on implantation, the biocomposite should have mechanical properties matching that of the host bone and it should bond to the host bone (bioactivity); and ideally the scaffold would resorb leaving only regenerated bone, with degradation products that are non-toxic. (10)

Some physical characteristics of the scaffolds must be considered when it is to be used in tissue engineering. In order to promote tissue growth, the scaffold must have large a large surface area to allow cell attachment. This is usually done by creating a highly porous polymer scaffold. In these scaffolds, the pore size should be large enough to allow cells penetration into pores, and the pores must be interconnected to facilitate nutrient and waste exchange. These characteristics (porosity and pore size) are often dependent on the method of scaffold fabrication.

Several methods have been developed to create porous scaffolds, including fiber bonding solvent, casting/particulate leaching, gas foaming, and the one which will be used in this work, phase separation.

Fiber bonding solvent

It consists in fibers bonded together in three-dimensions, which provide a large surface area for cell interaction and growth. The fibers can be attached to each other by immersion in a polymeric solution. When the solvent evaporates, the network of fibers is embedded in the solution. The composite is then heated and the polymer in solution melts first and fills all voids left by the fibers. This fabrication technique results in foams with porosities as high as 81%.

Although fiber bonding techniques produce highly porous scaffolds with interconnected pores that are suitable for tissue regeneration, it involve the use of solvents that could be toxic to cells if not completely removed. In order to extract these chemicals, the constructs must be vacuum dried for several hours, making it difficult to be used immediately in a clinical setting.

Solvent casting/particulate leaching

The first step in this process is to dissolve the polymer (PLLA or PLGA) in chloroform or methylene chloride and then cast it onto a petri dish filled with the porogen (e.g. salt). After evaporation of the solvent, the polymer/salt composite is leached in water for two days to remove the porogen. The resulting scaffold's porosity can be controlled by the amount of salt added, while the pore size is dependent on the size of the salt crystals. With 70%wt salt and above, the pores exhibited high interconnectivity.

With any solvent casting/particulate leaching procedure, organic solvents are used, which in many cases precludes the possibility of adding pharmacological agents to the scaffold during fabrication.

Gas foaming

In order to eliminate the need for organic solvents in the pore-making process, a new technique involving gas as a porogen has been introduced. The process begins with the formation of solid discs using compression molding with a heated mold. The discs are placed in a chamber and exposed to high pressure for three days, at which time the pressure is rapidly decreased to atmospheric pressure.

Porosities of up to 93% and pore sizes of up to 100 µm can be obtained using this technique, but the pores are largely unconnected, especially on the surface of the foam. While this fabrication method requires no leaching step and uses no harsh chemical solvents, the high temperatures involved in the disc formation prohibit the incorporation of cells or bioactive molecules and the unconnected pore structure make cell seeding and migration within the foam difficult.

Freeze drying

Freeze-drying, also known as lyophilization, is an industrial process which consists on removing water from a frozen sample by sublimation and desorption under vacuum. This process can be divided in three steps: freezing (solidification), primary drying (ice sublimation) and secondary drying (desorption of unfrozen water). (10) These steps are explained in the figure 3.10.

Freezing is the first step of freeze-drying. During this step, the liquid suspension is cooled, and ice crystals of pure water forms. As the freezing process continues, more and more water contained in the liquid freezes. The water that remains in the liquid state and does not freeze is called bound water.

The primary drying stage involves sublimation of ice from the frozen product. In this process,

i) heat is transferred from the shelf to the frozen solution through the tray and the vial, and conducted to the sublimation front

ii) the ice sublimes and the water vapor formed passes through the dried portion of the product to the surface of the sample

iii) the water vapor is transferred from the surface of the product through the chamber to the condenser

iv) the water vapor condenses on the condenser. At the end of sublimation step a porous structure is formed. Its pores correspond to the spaces that were occupied by ice crystals.

Secondary drying involves the removal of absorbed water from the product (the water which did not sublimate off). (10)

With the freeze-drying process, scaffolds up to 90% porous, with pores of approximately 100 µm, have been produced. This is a non toxic method to create porous scaffold: because no solvent is added to the mixture, so that no exterior intervention could pollute the scaffolds during the preparation phase.

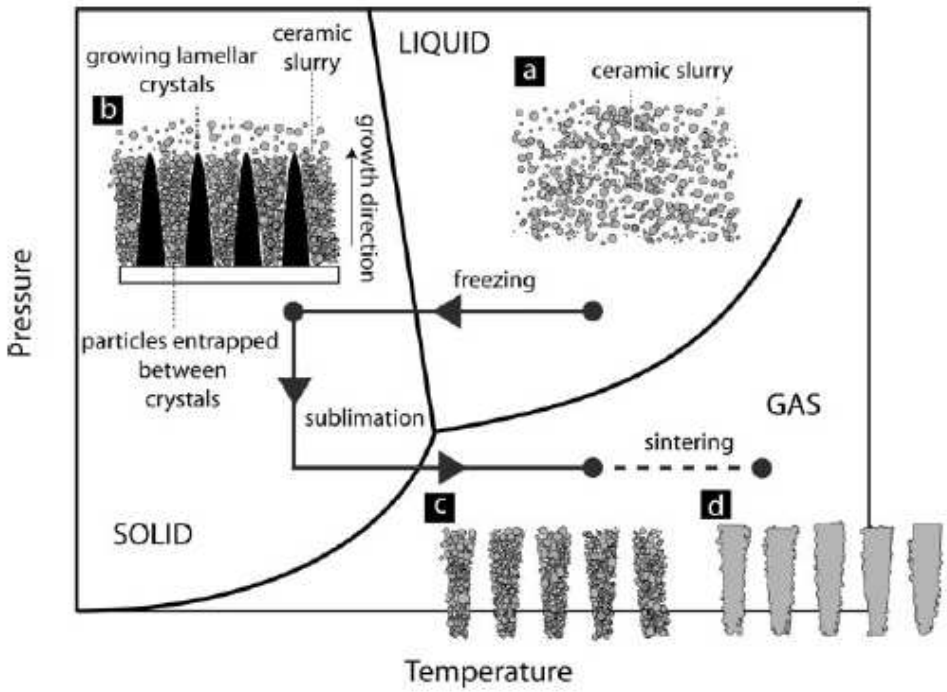

Fig 3.10: The four steps of freeze drying: slurry preparation, solidification, sublimation, and sintering (10)

4. Materials and methods

4.1 Materials

4.1.1 Preparation of the α-TCP

Alpha tri-calcium phosphate (α-TCP) is formed by the mixture of two components: calcium hydrogen phosphate ($CaHPO_4$) and calcium carbonate ($CaCO_3$).

The calcium hydrogen phosphate used was from Sigma-Aldric with a number of batch of 076K0064.

The calcium carbonate was also from Sigma-Aldric, opened the 24/07/08 and with a number of batch of 097K0042. The combination of both reactives weighted 150g to make easier the heating process (the jar in platinum can contain 150g maximum).

After mixing these two powders, the mixture was heated in oven 15h at 1400ºC (process in the figure 4.1), followed by a quench in air (in order to avoid the β-phase). Upon quenching (in order to avoid the β-TCP phase, less soluble than the α-TCP phase), the resulting material is milled to produce an adequate powder to create our scaffolds.

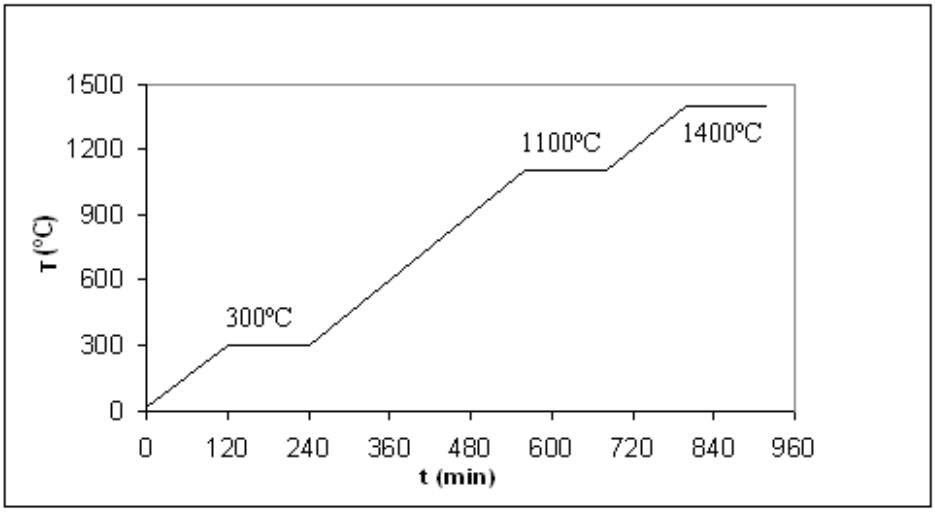

Fig 4.1: Heating process of the α-TCP

We prepared a well-determined size of α-TCP, named superfine, with the following a milling protocol: the powder was first milled in an agate ball mill with 10 balls (d=30mm) for 60 min at 450 rpm followed by a second milling for 40 min at 500 rpm,

and finally, with 100 small balls for 60 min at 500 rpm. The particle size distribution was analyzed by laser diffraction. In the figure 4.2, the process in order to get the α-TCP is resumed.

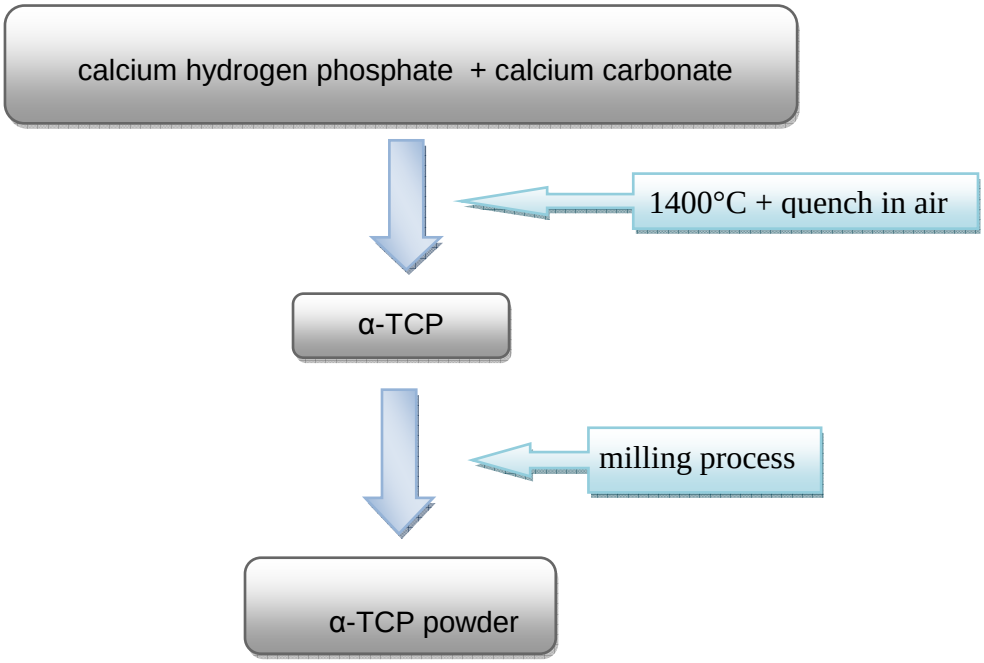

Fig 4.2: schema of obtention of the α-TCP

Once we get the α-TCP powder, we add 2% of hydroxiapatite precipitated (PHA) to enhance the grip reaction.

4.1.2 The gelatin caracteristics

In this work, a gelatin purchased was used: a jar of granules of 2-4mm. It is a gelatin of type B and with a bloom of 250.

4.1.3 Scaffold preparation

Two different types of scaffolds, respectively with organic matrix and inorganic matrix were prepared. The difference between them was the content of α-TCP. Scaffolds with organic matrix contained 0.5 wt % and 1.5 wt % of α-TCP whereas scaffolds with inorganic matrix had 10 wt % of α-TCP. The protocol used for their preparation was as follow. (11)

1) Heat a volume of water required to solubilize the amount of gelatin (5%wt) at 45ºC in a hot plate.

2) When the temperature of water is constant equal to 45ºC, add the gelatin in the water, maintain the temperature at 45ºC, under continuous stirring at 300rpm for 1h.

3) When all particles of gelatin are solubilized, add the α-TCP under continuous stirring at 300rpm, and at 45ºC and allow the powder to mix a specific time (1h, 2h, 4h, 6h).

Finally, the slurry was transferred into tubes made of PE, with dimensions of 23mm of diameter and 38mm of height. The volume considered was 12mL.

Then, several options are possible:

a) let tubes 10min at 25ºC (room temperature) and then put them in the freezer, at -20ºC, for 12h.

b) do the vacuum of the mixture, 10min, and then put them in the freezer, -20ºC, for 12h.

c) allow gelation occurs by putting tubes into ice cubes, 0ºC, 10min approximately (the most important thing is to see a change in the structure, it becomes more consistent, like a gel) and then, put them in the freezer, -20ºC, for 12h.

The samples were taken out from the freezer and lyophilized in a freeze-drier for 72h.

The dried scaffolds were crosslinked in a water solution of EDC-NHS. It was made dissolving 11.4µL of EDC and 0.37g of NHS in 100 mL of distilled water, with a molar ratio of 1:1.

This solution of EDC (Fluka, stored at -20ºC, lot: 1336449 41807006, purity >97.0%) and NHS (Aldrich, lot: S37955-516, purity >98.0%) was stored at 4ºC for 30min and then the scaffolds were put inside 24h at 4ºC.

After that operation, all the scaffolds are washed in Na_2HPO_4 for 10 minutes, two times, and then in distilled water 10 minutes, two times. The following flow chart (figure 4.3) resumes all the process of fabrication,

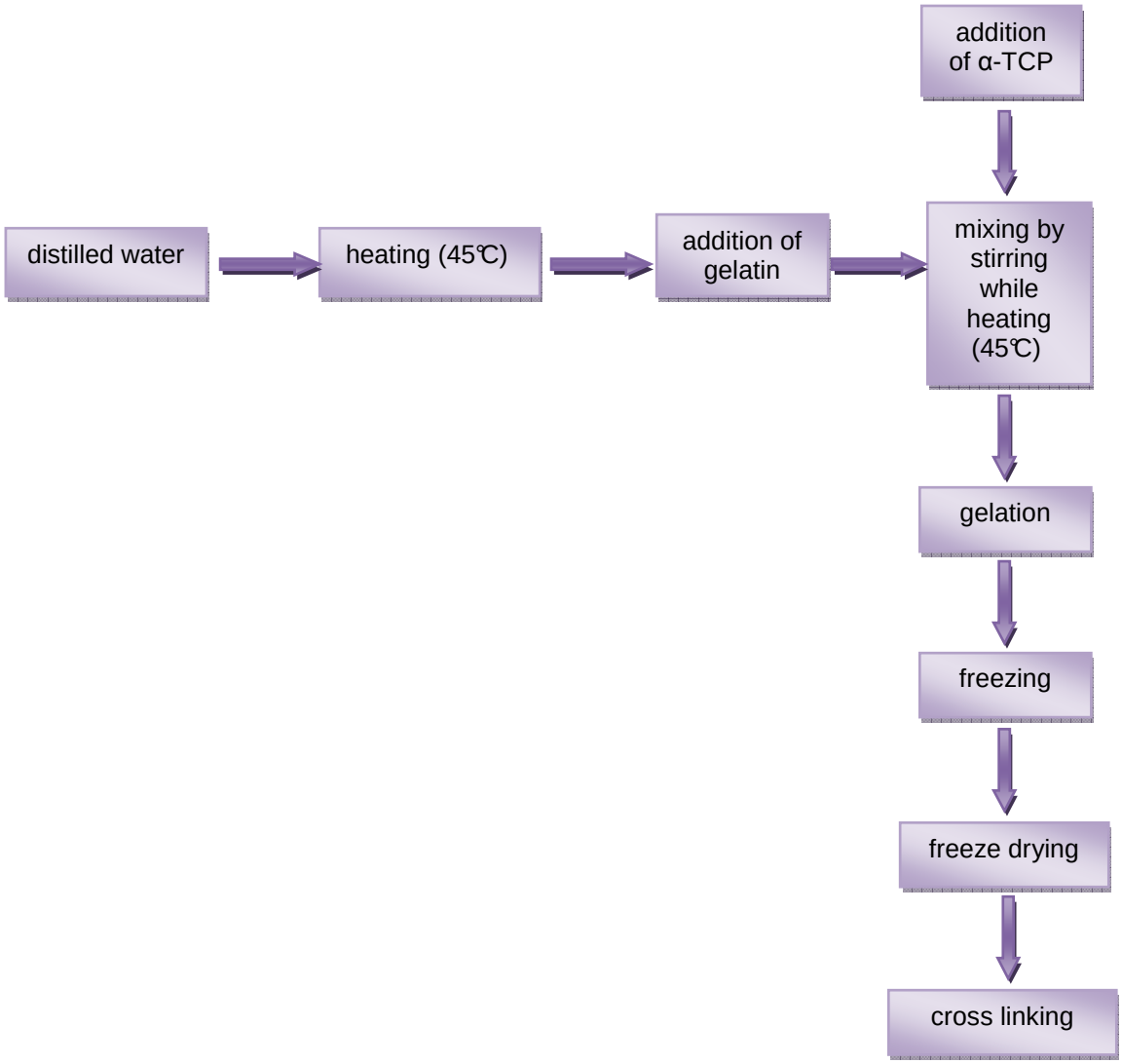

Fig 4.3: flow chart of the process

4.2 Methods

4.2.1 Laser diffraction particle size analyser

Laser diffraction is the most widely used technique for particle size analysis. This technique is easy to handle and really useful to analyse a broad size range in a variety of dispersion media. In this work, the machine used was the “Beckman Coulter LS 13 320” (figure 4.4).

In laser diffraction particle size analysis, a representative cloud of particles passes through a beam of laser light which scatters the incident light onto a Fourier lens. This lens focuses the scattered light on a detector array and, using an inversion algorithm, a particle size distribution is deduced from the collected diffracted light data. Since the size of the material under test is determined by measuring the angles at which the light is scattered, an accurate and consistent “angular zero” is crucial. If the laser beam is not accurately aligned, the light scatter pattern will be observed at the incorrect angle, and so that every measurement will be false. The LS 13 320 can do analysis across the widest dynamic range, from 40 nm to 2000 µm, in a single scan. The industry standard for reproducibility is 2%-4% but under ideal conditions, the LS 13 320, has better than 1% reproducibility.

Laser diffraction instrument uses Mie Theory as the basis of their size calculations. It is a complete analytical solution of Maxwell's equations for the scattering of electromagnetic radiation by spherical particles (also called Mie scattering). Mie solution is named after its developer German physicist Gustav Mie.

The measurement procedure is rather simple. In this work, analysis of a powder of α-TCP superfine was performed. A few grams of it were dissolved in ethanol (inert for our cement). Then, this solution was sonicated five minutes in order to disperse all particles to see them clearly during the analysis. A blank is doing before the measurement, and just after, the solution is introduced into the machine. The analysis is really quick, it takes only two minutes to give us the result diffractometer. (12)

Fig 4.4: Beckman Coulter LS 13 320 (12)

4.2.2 Freeze dryer

The freeze dryer, also called lyophilisator, is the most important machine in this work: it permits to create macroporosity in the scaffolds. Lyophilisation comes from Lyo, which means solvent, and philo, friend in greek. It is a drying of a product previously frozen, done at low temperature, which allows sublimation, in a vacuum atmosphere. This freeze drier Cryodos by Telstar (figure 4.5) has a standard 8-connection manifold and a corresponding two-stage vacuum pump. The unit is supplied with a two-stage vacuum pump, located outside the freeze dryer body. All the critical parts are made out of AISI 316L stainless steel. (13)

Fig 4.5: Freeze dryer "Cryodos", Telstar (13)

The basic rules that define lyophilisation are set on the triple point diagram of water.

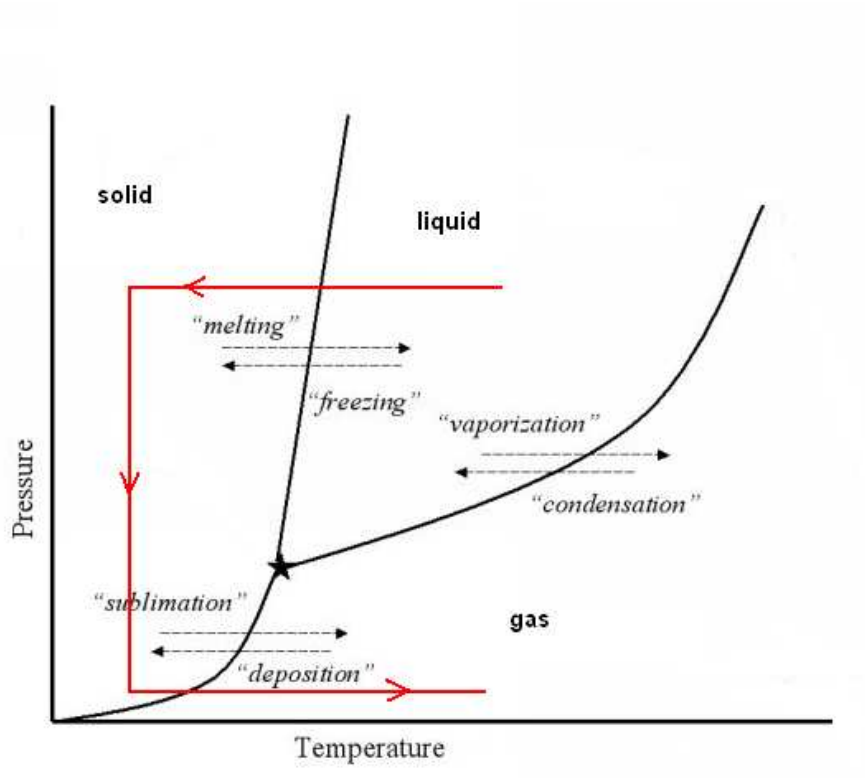

Fig 4.6: schema of the triple point of the water state

As we see in the figure 4.6, the slurry is freezing first. Fusion has to be avoid during all the process. The pressure goes down under the pressure of the triple point (6.1mbar) and then the temperature increases in order to sublimate the product. The water vapor emitted solidifies in the condensator (to avoid contamination of the product by water vapor) and during the ultimate phase, this freeze melts and is eliminated as liquid water.

The vacuum is processed, the temperature and pressure decrease until approximately -80ºC and 1mbar, and then sublimation occurs.

The moment when the drying is over can only be determined by various experiments, analysing the aspect, cutting the material to see if there remains humidity inside… The final product is a dried solid body, with a porous structure.

Once the process is finished, vacuum has to be cut to re-established the atmospherical pressure. This step has to be really slow to avoid catching of particles by the machine. (13)

The scaffolds are placed, in a frozen state, in bottles of glass. This step comes after the freezing step because the solvent (water) needs to be frozen before. The valve is turned on to allow the process to begin. Time of processing is approximately 36 hours.

4.2.3 Scanning electron microscopy

To characterize the microstructure of the scaffolds, a Scanning Electron Microscope (SEM) JEOL JSM-6400 was used. The observation was performed with a difference of potential of 15kV. The following schema (figure 4.7) presents the SEM composition.

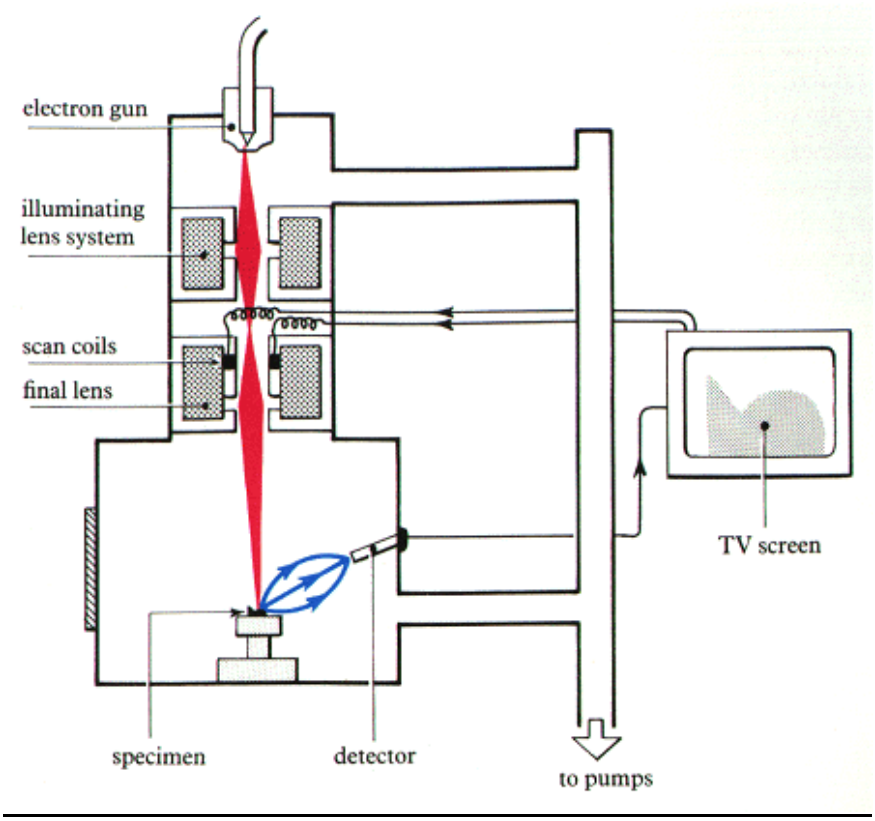

Fig 4.7: Schema of a scanning electron microscope (14)

Process

The electron beam comes from a tungsten filament. This filament is a loop which works as the cathode. A voltage is applied to the loop, causing a heat. The anode, which is positive with respect to the filament, forms powerful attractive forces for electrons. This causes electrons to accelerate toward the anode.

They was then condensed by a condenser lens, and focused as a very fine point on the sample. The scan coils are energized (by varying the voltage produced by the scan generator) and create a magnetic field which deflects the beam back and forth in a controlled pattern.

The electron beam hits the sample, producing secondary electrons from the sample. These electrons are collected by a secondary detector or a backscatter detector, converted to a voltage, and amplified.

The amplified voltage is applied to the grid of the CRT and causes the intensity of the spot of light to change. The image consists of thousands of spots of varying intensity on the face of a CRT that correspond to the topography of the sample.

The importance of the vacuum

When a SEM is used, the column must always be at a vacuum. There are many reasons for this. If the sample is in a gas filled environment, an electron beam cannot be generated or maintained because of a high instability in the beam. Gases could react with the electron source, causing it to burn out, or cause electrons in the beam to ionize, which produces random discharges and leads to instability in the beam. The transmission of the beam through the electron optic column would also be hindered by the presence of other molecules. Those other molecules, which could come from the sample or the microscope itself, could form compounds and condense on the sample. This would lower the contrast and obscure detail in the image.

The scaffolds were cut to be collocated on a patch of copper (figure 4.8), and stuck with carbon ribbon to assure the conduction of electrons through the scaffolds. Colloidal silver liquid and a sputter coating (gold in this case) were also added both on the surface of scaffolds and the patch to enhance this conduction, and to assure the best image as possible with the SEM. (14)

Fig 4.8: Patch with 6 samples with gold sputter coating

4.2.4 Helium pycnometry

Helium pycnometry was used to evaluate the porosity of the samples, by calculate their skeletal density. It is the intrinsecal density of the sample; the volume has no effect on it.

Samples were analyzed by a gas displacement pycnometer, AccuPyc 1330 Pycnometer from Micromeritics (figure 4.9), which measures the volume of solid objects of irregular or regular shape whether powdered or in one piece. Helium is used as a displacement medium. The sample is sealed in the instrument compartment of known volume, helium is admitted, and then expanded into another precision internal volume. The pressure before and after expansion are measured and used to compute the sample volume. Dividing the volume by the sample weight gives the helium displacement density. (15)

$$\rho_{skeletal} = \frac{sample\ mass}{skeletal\ volume} \qquad \text{(eq.1)}$$

The samples were disposed in chambers of 1 or 3.5cm^3, according to their size.

Fig 4.9: AccuPyc 1330 pycnometer from Micromeritics

To calculate the percentage of closed pores and connected pores, the following formulas were used.

The bulk density is the quotient of the mass of all particles of the sample and the volume of the sample (even the spaces between particles and pores). So, it is not an intrinsecal property because it depends on the porosity of the material.

To get these other densities, the real and the bulk, some calculations are necessary.

$$\rho_{theoretical} = (\rho_{\alpha-TCP} \times \%_{\alpha-TCP}) + (\rho_{gelatin} \times \%_{gelatin}) \qquad \text{(eq. 2)}$$

$$\rho_{bulk} = \frac{sample\ mass}{sample\ volume} \qquad \text{(eq. 3)}$$

Closed pores ratio has to be a well-known value. If it is too high, the passage of cells or proteins into the scaffold could be compromised.

$$\%_{close\ pores} = \rho_{bulk} \times (\frac{1}{\rho_{bulk}}) - (\frac{1}{\rho_{real}}) \times 100 \qquad \text{(eq.4)}$$

4.2.5 X-rays diffraction

This method is really useful to determine phases into a scaffold. Indeed, the most important thing to studied is the speed and the rate of the transformation of α-TCP into CDHA.

The equipment was a geometric diffractometer Bragg-Brentano PANalytical X'Pert PRO alpha1.

The transformation from α-TCP to CDHA can be evaluated by the observation of specific peaks on the patterns which caracterize each phase.

4.2.6 Infrared spectroscopy

Infrared vibrational spectroscopy is a technique which can be used to identify molecules by analyze their bonds. Each chemical bond in a molecule vibrates at a frequency which is characteristic.

The vibrational frequencies of most molecules correspond to the frequencies of infrared light. In this technique, a spectrum of all the frequencies of absorption of a sample is recorded. This can be used to gain information about the sample composition in terms of chemical groups present and also its purity.

4.2.7 Compression test

Compression tests were processed with an electromechanical universal machine Adamel Lhomargy DY 34 (figure 4.10).The sample is settled on a plate and a piston goes down to compress it in the axial direction. The speed is defined at 1mm/min and the loading cell which applies the force on the sample is 10kN.

From the data given by the machine, we can deduce the stress-strain curve and find the young modulus by the Hooke's law:

$$E = \frac{stress}{strain} = \frac{\sigma}{\varepsilon} \qquad \text{(eq. 5)}$$

$$\sigma = \frac{F}{S} \qquad \text{(eq.6)}$$

F is the force applied to the sample and S is the cross section area.

$$\varepsilon = \frac{L - L_0}{L_0} \qquad \text{(eq.7)}$$

L is the length of the scaffold after the test and L_0 is the initial length of the scaffold.

Scaffolds with adequate dimensions were prepared for these series of tests. They had 10mm of height and a diameter of 5mm. For each scaffold, several tests were done.

Fig 4.10: Compression test machine Adamel Lhomargy DY 34

5. Results and discussion

5.1 Characterization of the α-TCP powder

Results from particle size distribution (Figure 5.1) of α-TCP shows that the average size of particles is 4.5μm and more than 90% of them are under 10μm.

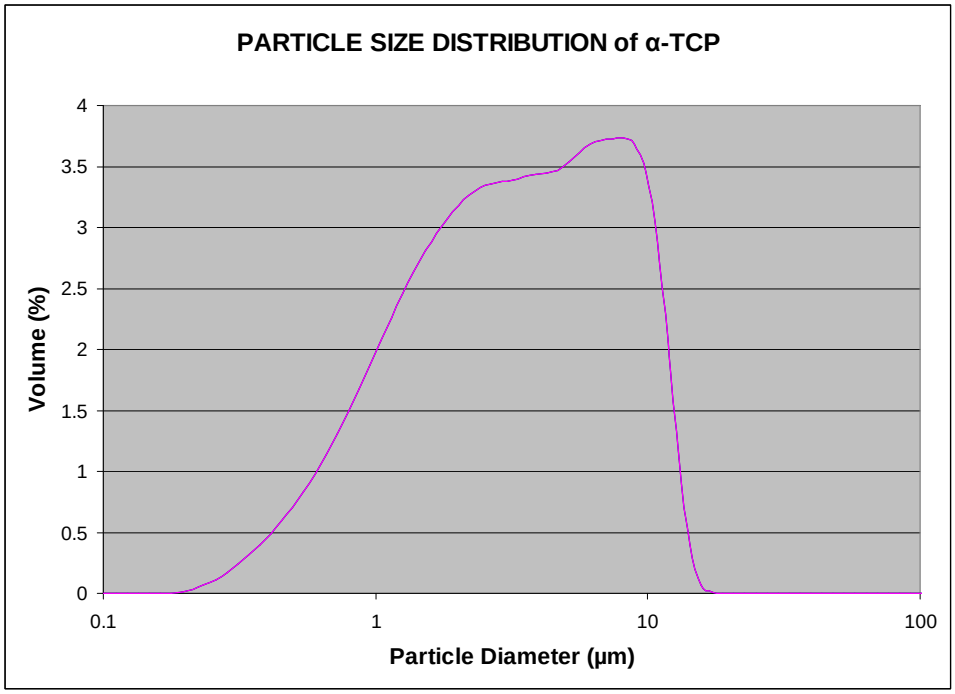

Fig 5.1: Particle size distribution in the α-TCP superfine powder

The particle size of this α-TCP powder is considered to be relatively small.

Indeed, this is a real important parameter which influences the interaction with gelatin during the stirring.

5.2 Optimization of the fabrication process of scaffolds with organic matrix

Our goal was to create scaffolds composed of gelatin and α-TCP, with a structure comparable to the existing bone. In order to produce scaffolds with acceptable microstructure, with the required porosity, the process of fabrication needed to be clearly defined and improved. This process, in the case of scaffolds of organic matrix, already exists, and was explained by Kim and Knowles (16). This article was used as a reference and the procedure was optimized. The following points were examined.

i) optimization of reactives proportions

ii) the heating time of the slurry solution

iii) the effect of doing or not the vacuum into the slurry

iv) the influence of the gelation

5.2.1 Proportion of reactives

Right and well defined proportions for our reactives, gelatin and α-TCP, had to be found. The article of Kim and Knowles (16) was followed and same proportions were used: 5 wt % of gelatin with 0.5 wt % of α-TCP and 5 wt % of gelatin with 1.5 wt % of α-TCP.

Kim created scaffolds with organic matrix with 5 wt % of gelatin, and respectively 0.5 wt %, 1.5 wt % of α-TCP. In this work, we followed those proportions, but we also created scaffolds with inorganic matrix, which have never been studied or created before.

Proportions into bones were examined: 64% v/v of inorganic phase, hydroxyapatite, and 36% v/v of organic phase, collagen. In this study, the inorganic phase resulting from the hydrolysis of α-TCP is Calcium Deficient HydroxyApatite (CDHA) and organic phase is gelatin. (16)

	organic phase (%v)	inorganic phase (%v)
bone (17)	36	64
gelatin 5 wt % +α-TCP 0.5 wt %	95	5
gelatin 5 wt % +α-TCP 1.5 wt %	88	22
gelatin 5 wt % +α-TCP 10 wt %	52	48

Fig 5.2: table of the proportions of organic and inorganic phases into bones and the scaffolds created

For the scaffolds with organic matrix, a small amount of α-TCP was added, and the gelatin acted as a binder. For the samples with inorganic matrix, it is the α-TCP which acted as a binder. For these specific samples, we are closer to the real proportions present into bones, as we see in the figure 5.2.

In the figure 5.3, a general view of a scaffold is shown.

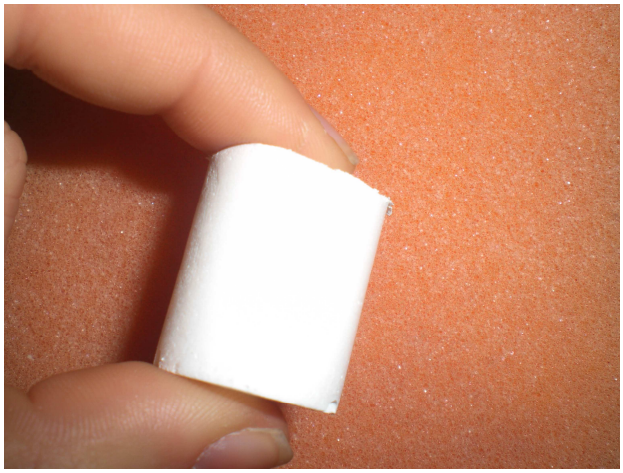

Fig 5.3: scaffold of gelatin and α-TCP

5.2.2 Experimental conditions

5.2.2.1 Time of heating

Microstructure

Different times of heating (while stirring) the slurry (dissolved gelatin containing α-TCP particles) were also studied. A first experiment was done with two types of scaffolds with organic matrix: 5 wt % of gelatin with 0.5 wt % of α-TCP and 5 wt % of gelatin with 1.5 wt % of α-TCP. These two slurries were controlled at 1h, 2h, 4h and 6h of heating at 45ºC, with a stirring speed of 300rpm. The resulting cross sections were then observed by scanning electron microscopy (SEM).

	0.5 wt % of α-TCP	1.5 wt % of α-TCP
2h	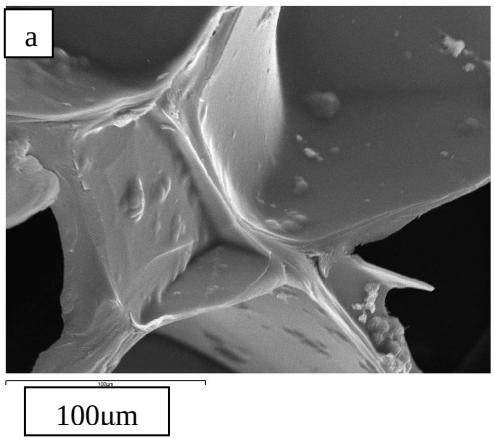	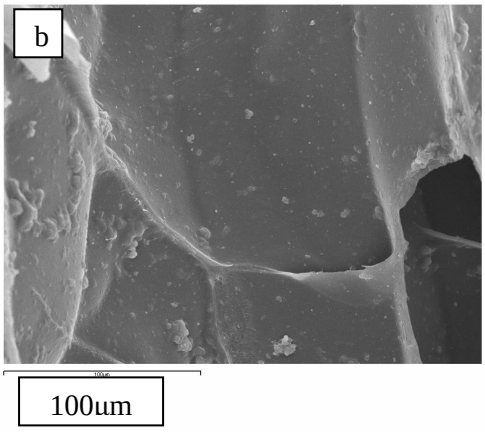
6h	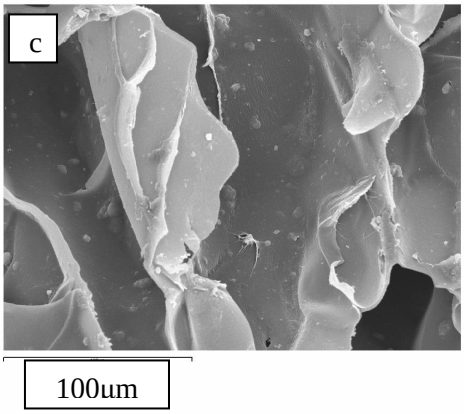	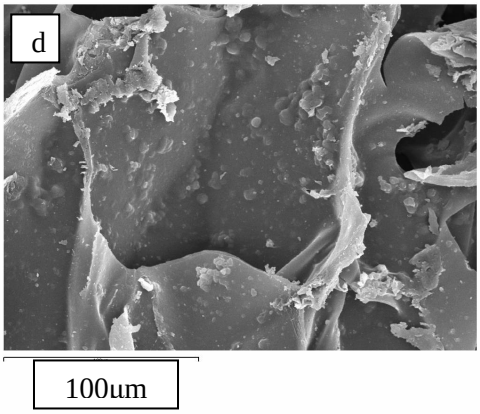

Fig 5.4: samples observed by SEM: (a), (c) gelatin 5 wt % + α-TCP 0.5 wt %, respectively 2h and 6h of heating, (b), (d) gelatin 5 wt % + α-TCP 1.5 wt %

The observation of the SEM images in the figure 5.4 reveals that the longer the time of heating while stirring, the more particles are dispersed in the gelatin matrix. There are more particles after 6h than after 2h for both concentrations of α-TCP, when we look at the SEM pictures, figure 5.4.

Before putting our samples in the freezer, we have noticed that when the protocol was done with the options a) or b) (as explained in the part 4.1.3), letting the samples at room temperature without doing the vacuum or with a vacuum, there was sedimentation of particles in the bottom of the tubes for both cases, just after we stop the magnetic stirrer in the slurry.

It can be assumed that with less time of stirring, particles of α-TCP are more agglomerated (not very dispersed) in the gelatin matrix. Indeed, particles seen in the picture a (2h) of the figure 5.4 have a larger diameter than those in the picture c (6h). This diameter could be the one of several particles agglomerated.

It means that the incorporation of the particles of α-TCP was not complete. There was always sedimentation because the density of the α-TCP particles is higher than the one of the liquid phase and this effect of agglomeration.

The time of heating, while stirring, influences the incorporation and the interaction of the α-TCP particles with the gelatin. This is a question of wettability, between α-TCP particles and the gelatine matrix. (18)

Consequently, with increasing the mixing time, the particles of α-TCP interact with the gelatin matrix to develop bonds and are incorporated to the gelatin matrix, and are not collapsing at the bottom of the tube.

The percentage of α-TCP sedimented must be considered in order to evaluate the real amount of α-TCP incorporated in the scaffold.

Upon cutting the bottom part of the scaffold (where α-TCP particles sedimented), the remain scaffold was weighted and then burned off at 800ºC (2h) to eliminate the gelatin. At the end, only the α-TCP remains. The sample was weighted again and the loss of α-TCP in the sample can be evaluated.

The resulting powder was then analyzed by infra-red (figure 5.5), to see if the gelatin entirely burned during calcination.

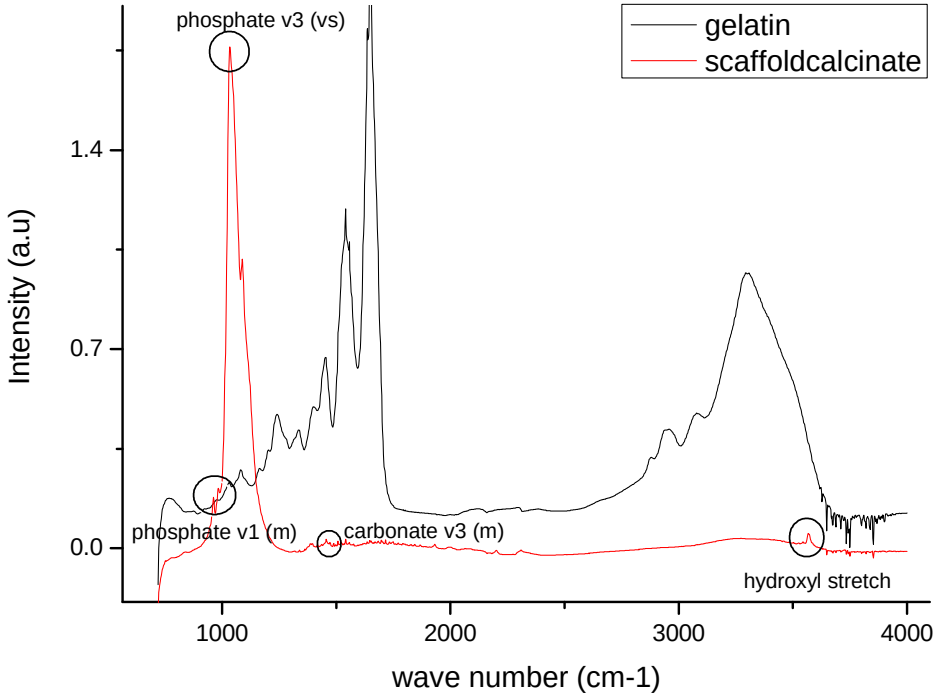

Fig 5.5: Infra-red pattern of the gelatin and a scaffold of gelatin and α-TCP

In the figure 5.5, infra-red patterns of gelatin and of the remaining powder are introduced.

The gelatin (black curve) exhibits the specific bands of its structure. The powder (scaffold calcinated, red curve) shows other bands, clearly distinct from those of the gelatin. These bands stand for the PO_4^{3-} , CO_3^{2-} and OH^-. It can be said that there is not gelatin remaining and that it burned totally during calcination.

With the mass before calcination and after it, we are able to quantify the loss of α-

TCP during the heating while stirring time.

For the scaffold obtained after 2h of heating while stirring, the loss is 54.6% in mass, for a sample with 0.5wt% of α-TCP.

Composition

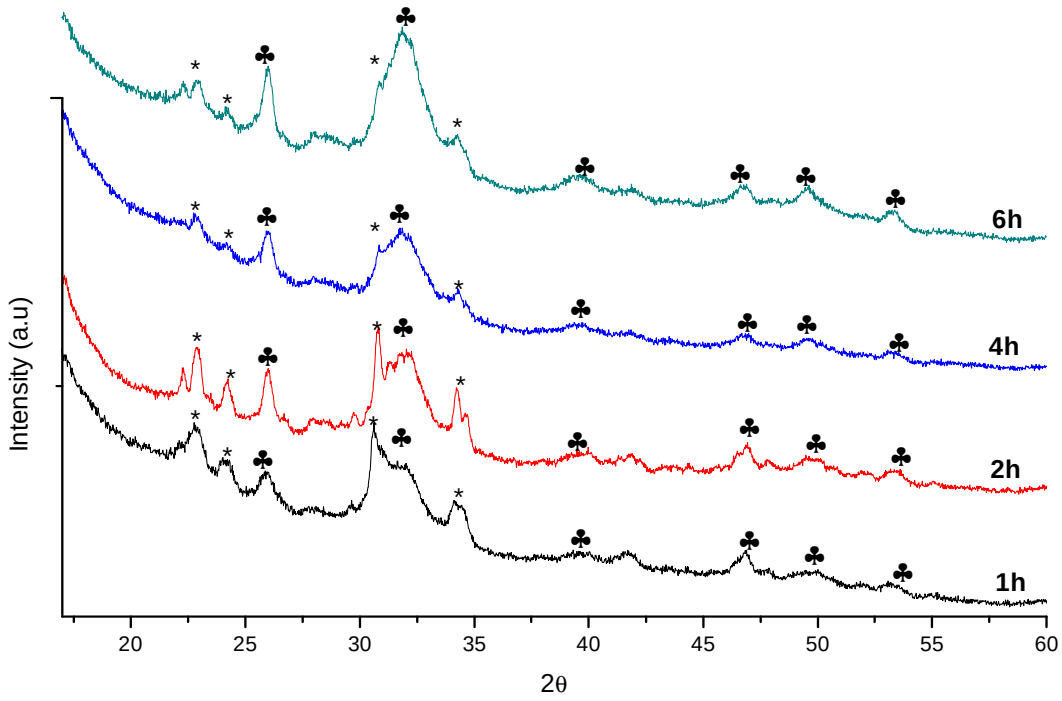

Fig 5.6: XRD pattern of scaffolds made of gelatin and TCP after 1h, 2h, 4h and 6h of mixing followed by vacuum

In order to see the chemical composition of the scaffolds with organic matrix, X-rays diffraction was processed on the same samples (1h, 2h, 4h and 6h) as we can see on the pattern, figure 5.6. Here, we wanted to control the amount of hydroxyapatite created with respect of the time of heating while stirring.

Those curves give some interesting results. We can easily see the two inorganic

components which are α-TCP (all peaks with *) and HA (all peaks with ♣). For the identification, the PDF-file number 09-0348 and 09-0432 were used to index α-TCP and HA respectively (see Annex A-1).

After one hour of mixing, α-TCP is the dominant phase in the scaffold. The scaffold mixed two hours shows a relative equivalence between the two phases. After 4h, HA becomes more present in the scaffold. Finally, at 6h, HA is becoming the dominant phase and there is only a little fraction of α-TCP remaining. The phenomenon of transformation in HA is rather fast.

For our scaffolds, the best option is to have the more α-TCP as possible to create links during freeze-drying phase. So, the best choice seemed to be a 2h mixing time.

5.2.2.2 Effect of the vacuum

The vacuum of the slurry was done just after the heating while stirring the slurry and before putting them in the freezer. Vacuum was done placing the samples in a desecator connected to a pump.

All air bubbles which were entrapped in the mixture, due to the stirring, will be removed. With vacuum, scaffolds have a better aspect, but also a porosity relatively homogeneous, because of the absence of air bubbles while freezing.

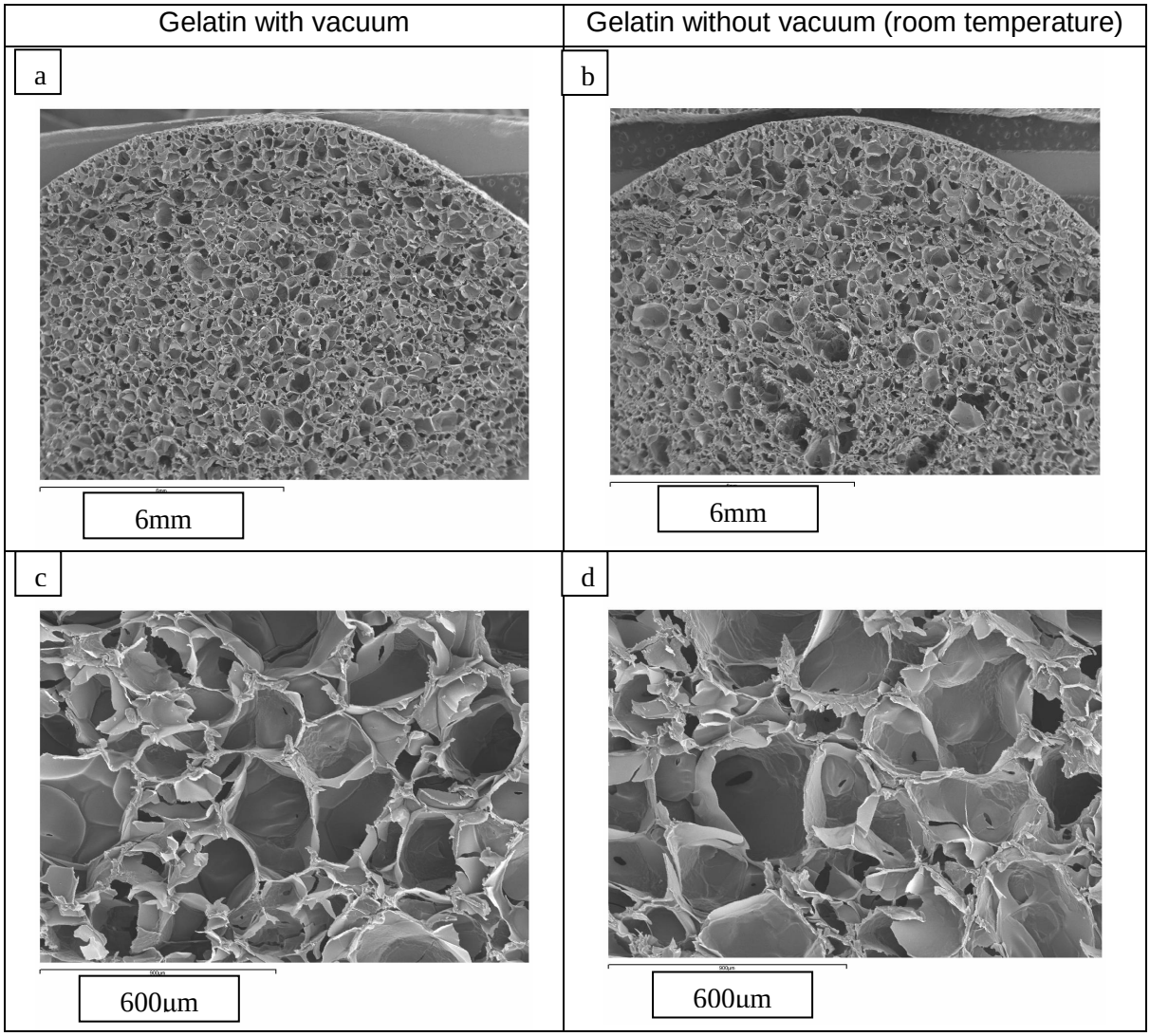

Fig 5.7: SEM images: (a)(c) gelatin 5wt% with vacuum, (b)(d) gelatin 5wt% without vacuum

In these SEM pictures (figure 5.7), and especially (a) and (b), as we can see the scaffold in a general view, gelatin has a porosity more homogeneous doing the vacuum than without doing it (room temperature).

The figure 5.8 shows the influence of the vacuum on the microstructure of a scaffold with 1.5wt% of α-TCP.

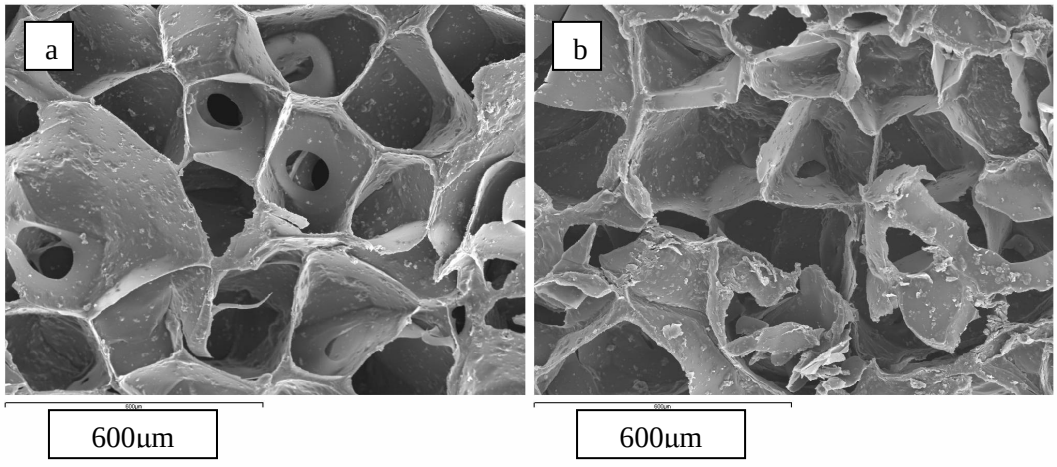

Fig 5.8: SEM images: (a) gelatin 5wt%+α-TCP 1.5wt% with vacuum, (b) gelatin 5wt%+α-TCP 1.5wt% without vacuum

With this diagram, it can be conclude that doing the vacuum before freezing the scaffolds has an important effect especially on the ratio of interconnected pores.

When vacuum is done inside the slurry, all the air is removed from it and formation of pores, especially connected pores, is easier, which consequently reduce the rate of closed pores.

But, even if vacuum has many positive aspects, it cannot avoid the sedimentation of particles at the bottom of tubes, which remains a problem.

5.2.2.3 Effect of gelation

Gelation is done after the heating and stirring of the slurry, instead of the room temperature or vacuum step. It is an alternative to the vacuum: we have observed that sedimentation still occurred doing it, so we wanted to try another option. Gelation of our scaffolds was principally processed to avoid particles deposition at the bottom of the mould, and make the slurry more homogeneous before freezing it at -20ºC.

Cooling down to the gel point of the gelatine, the slurry coagulated to form a white body. To do that, different methods were tried: gelation in room temperature (25ºC), in a box full of ice (0ºC), in cold water with ice cubes (10ºC). In all cases, gelation was allowed under continuous stirring. The apparent viscosity, directly linked to the gelation, appears to change at 20ºC. It appears that the only difference between these 3 techniques was the speed of gelation. We choose to do gelation always in a box full of ice cubes, to make the process faster.

The result was what we expected: the gelation under stirring entrapped the particles and avoided sedimentation at the bottom of tubes, which means no loss of α-TCP. In the following SEM images, general view (figure 5.9) and detailed view of the microstructure (figure 5.10) of a sample with gelation applied and sample without gelation are presented.

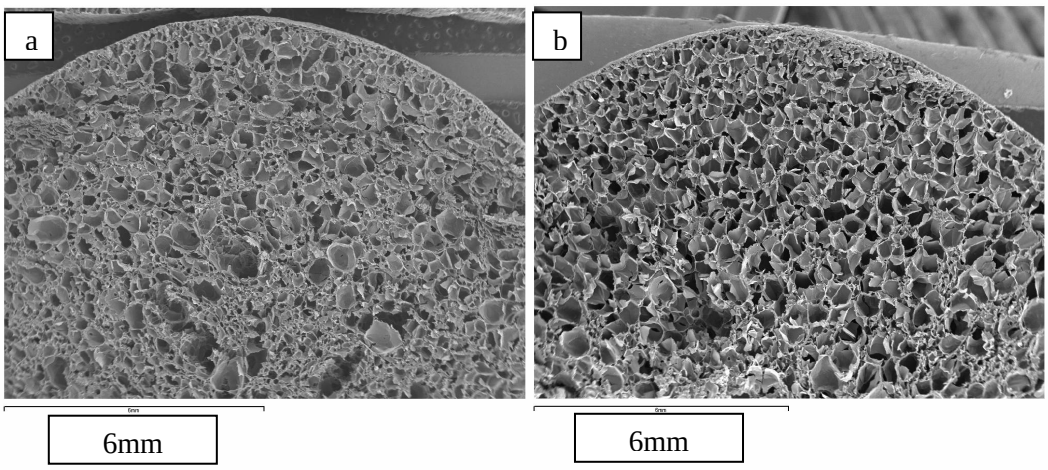

Fig 5.9: gelatin 5wt% + α-TCP 1.5wt%, (a) sample no gelified, (b) sample gelified, general view

In those pictures, there is clearly an open porosity when gelation process is applied to the sample (b). For the sample frozen without gelation (a), the interface exhibits a closed microstructure, resulting in poor pore interconnectivity. Such architecture is not suitable for tissue engineering, as would not allow cells to pass through.

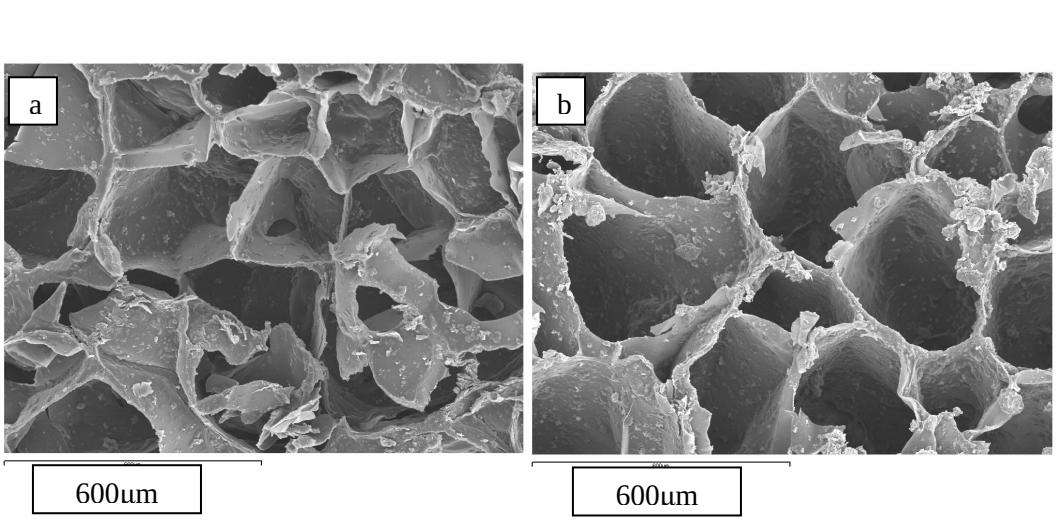

Fig 5.10: gelatin 5wt% + α-TCP 1.5wt%, (a) sample no gelified, (b) sample gelified, detailed view of the microstructure

In figure 5.10.b, open porosity is evident in the microstructure.

For a sample previously gelified, the structure forms a sort of block. This structure is already opened, thanks to its gel state. Consequently, there are more connected pores created during gelation than during vacuum or room temperature processes: the microstructure is much better with gelation. (19)

5.2.2.4 Freezing

Before freeze drying, samples had to be frozen. The freezing process was always performed in the freezer at -20ºC, and the only parameter that was studied was the location of the samples into it.

They were located inside this cavity for 12h. The first results weren't acceptable because of a heterogeneous structure. The base of all the scaffolds was like a stone and it seemed to be a tubular growth while cutting it. This problem appeared because they were placed directly on the ice, and this way, the freezing couldn't be uniform. We had a unidirectional direction of pores because the freezing went from the base of the tube (figure 5.11)

Fig 5.11: scaffolds exhibiting freezing defects

So that, samples were elevated onto a plastic structure (with some holes inside, to let cold pass through it). By this method, the problem of heterogeneous structure was solved.

5.2.2.5 Cross linking

Cross-linking is the last step of the process. It comes after lyophilisation of the scaffolds, which are already in a solid state. If samples are not cross-linking, scaffolds would dissolve in the body.

Among all crosslinked agents, EDC was chosen in this experiment. However, glutaraldehyde is the agent most frequently used in biochemistry applications. The main drawback of glutaraldehyde is its toxicity. Indeed, this experiment was driven in a way of respect of the environment and health.

Crosslinking is done by activating the carboxylic groups of the glutamic and aspartic acid residues in collagen.

Figure 5.12 introduces scaffolds with organic matrix crosslinked. The sample has become more compact and its consistence has increased.

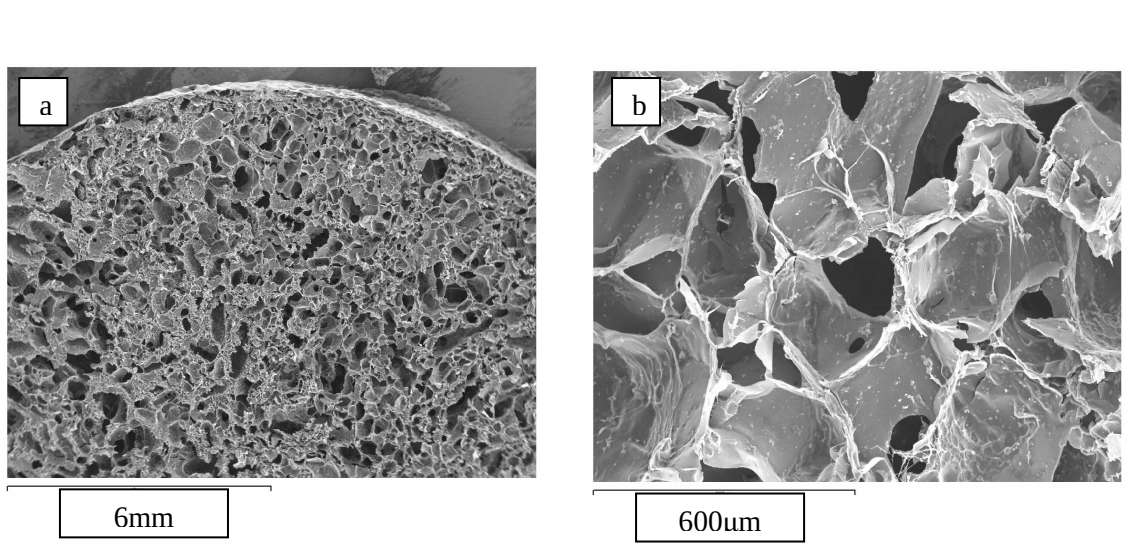

Figure 5.12: Scaffold with organic matrix (α-TCP1.5 wt %): (a) general view, (b) detailed view

When same proportions of crosslinking agents were tried for the cross-linking of scaffolds with inorganic matrix, these one collapsed once they were put into the solution. Another molar ratio had to be found. A compromise was then decided: the molar ratio will be the same 1:1 but the quantity of the two components (EDC, NHS) is then multiplied by two and the solution had to be cold before putting these scaffolds inside.

So, each time a crosslinking was necessary for an inorganic scaffold, the solution of EDC-NHS was placed in the fridge 20 minutes and scaffolds are immersed in it during 24h. The reason of putting it in a cold environment is to avoid the degradation of these special scaffolds which have less cohesion than the organic ones.

5.3 Scaffolds with organic matrix

5.3.1 Morphology

In this section, morphologies of scaffolds with organic matrix will be presented. Figure 5.13 shows the SEM morphology of pure gelatin.

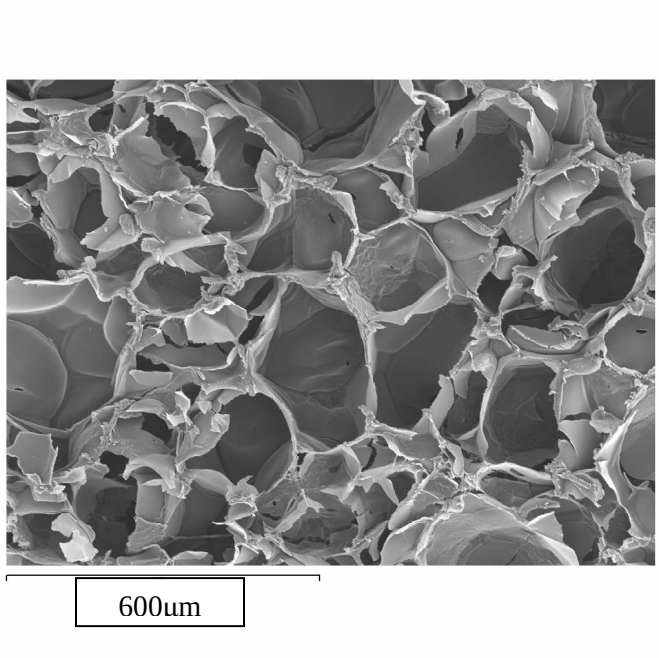

Fig 5.13: gelatin 5 wt %

It showed a well-developed porous structure. All scaffolds were made using gelation process. Here, the pore size is approximately 300µm. Indeed, cells can colonize a porous structure if pore size is higher than 100µm. So, cell colonization is possible: cells can enter into pores.

This is a good point but there is a problem when porosity is too large. Indeed, the mechanical could be affected. The freezing step has to be controlled, in the fact that it is during this time that pore size is defined. The freezing needs to be slow. A rapid cooling rate could affect the microstructure and this is very clear seeing these two different pictures. When the freezing kinetics is increased, the solidification front speed increases, and the width of the pores and is drastically affected. As shown in those pictures, the structure can be varied. The faster the freezing rate, the less homogeneous is the microstructure. (20)

The figure 5.14 shows a scaffold with organic matrix made of gelatin (5 wt %) and α-TCP (0.5 wt %).

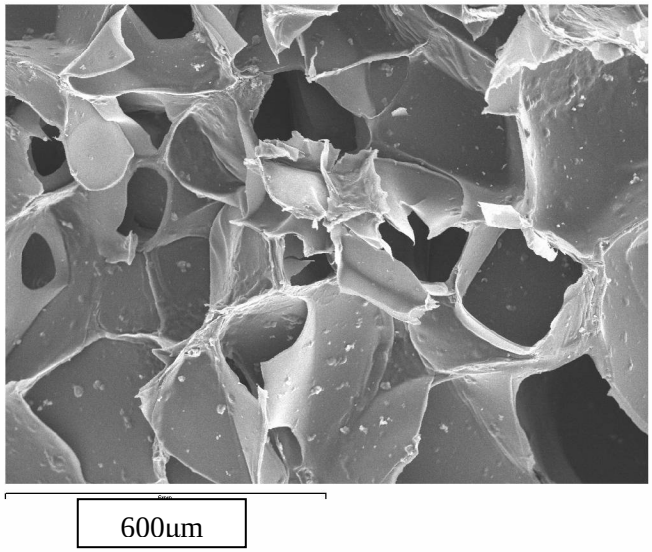

Fig 5.14: gelatin 5 wt % + α-TCP 0.5 wt %

Particles of α-TCP can easily be seen on the gelatin matrix. The average diameter of pores is 200μm, which means cells can enter into them. Some holes can be observed in this porous network. The addition of α-TCP may explain that phenomenon, and those holes should have been created during the stirring period. This gives a new criterion to the porous structure: now we have connected pores. This is a crucial point to make easier the circulation of cells in the implant. The more the scaffold has an interconnected porosity, the best is for the implantation and living into the body. (16)

A scaffold made of gelatin (5 wt %) and this time with 1.5 wt % of α-TCP is presented in this figure 5.15.

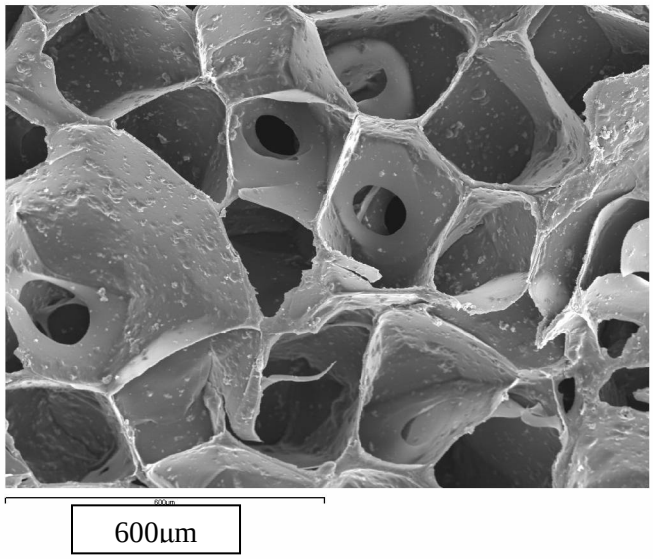

Fig 5.15: *gelatin 5wt% + α-TCP 1.5wt%*

There are more particles of α-TCP on the gelatin matrix, which is obvious. But there are also more holes and consequently more interconnected pores. The average diameter of pores is similar to the scaffold made with 0.5 wt % of α-TCP.

Although the α-TCP was added initially as powders in the microrange size they agglomerated to form particles within the gelatin sol with sizes of 1-2 mm.

5.3.2 Phase and structure

In the figure 5.16, there are 3 x-rays diffraction patterns of 3 different scaffolds: gelatin, gelatin with 0.5wt% of TCP and gelatin with 1.5wt% of TCP

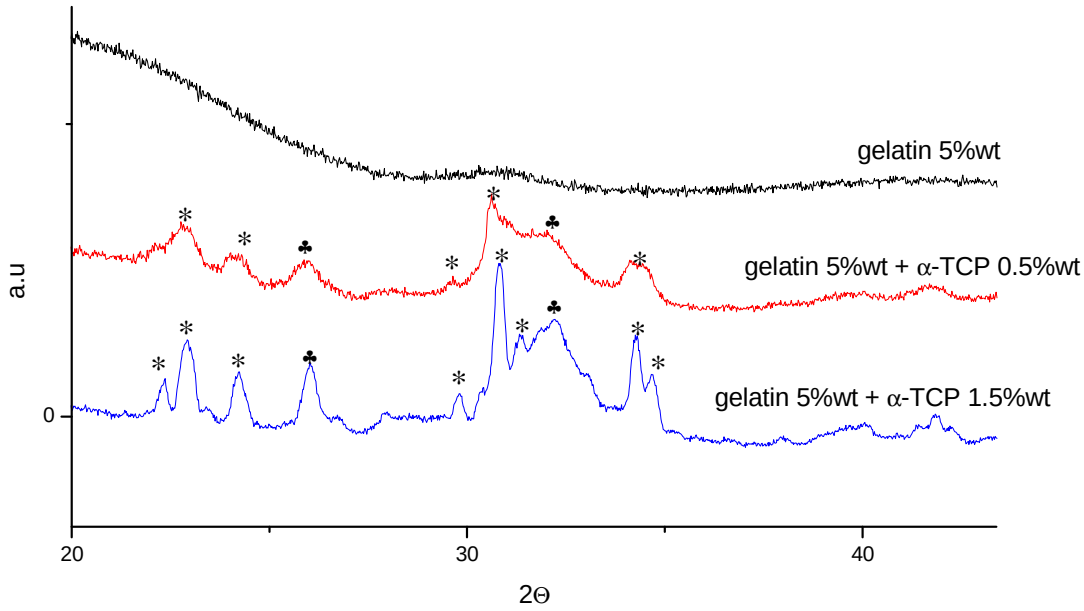

Fig 5.16: XRD pattern of scaffolds made of gelatin and TCP at different composition

. They were all mixed during 2h. We can see it on all the curves (all scaffolds contain gelatin in the same proportions, 5 wt %). The stars represent the α-TCP peaks and the clovers stand for HA. With 1.5 wt % of α-TCP, peaks of α-TCP are clearly higher than for 0.5 wt %, which is logical. For the identification, the PDF-file number 09-0348 and 09-0432 were used to index α-TCP and HA respectively (see annex A-1).

5.3.3 Porosity

The porosity of the scaffolds has been deeply studied. The figure 5.17 shows the percentage of closed pores of the sample with 0.5 wt % of α-TCP.

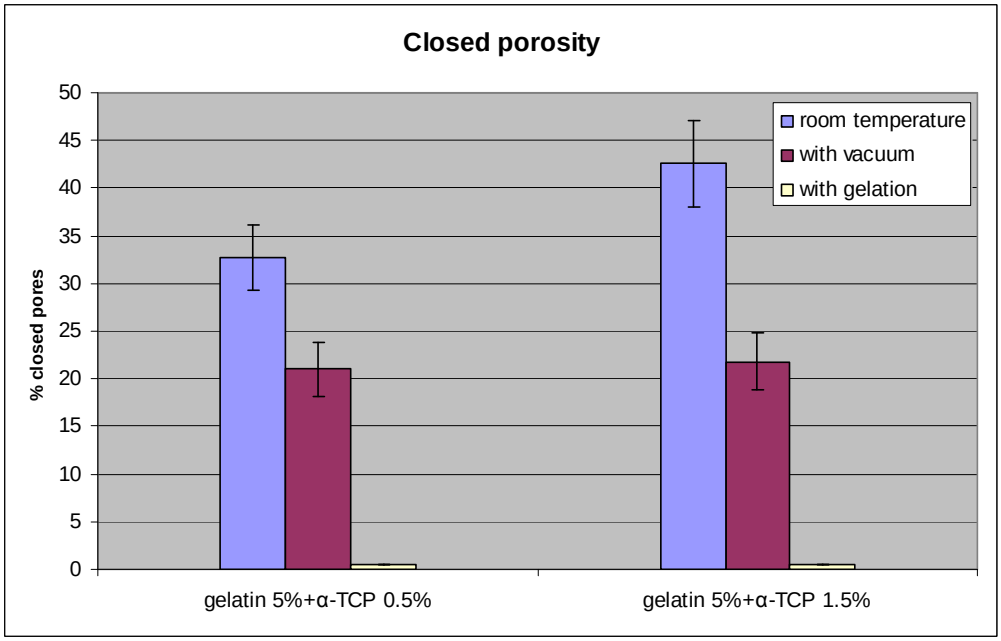

Fig 5.17: Closed porosity for gelatin 5 wt % +0.5wt% α-TCP

We can see the effect of the different methodologies tried in order to have the less closed porosity as possible: upon mixture of the two phases, the scaffold was either let at room temperature, submitted to vacuum or to the gelation. Closed porosity must be avoided because it is useless in the medical application: the implant has to be colonized by cells and in this type of porosity, cells cannot pass through the scaffold.

At room temperature, the percentage of closed pores is around 32% which is a really high value for the future application of these scaffolds (permit the transport of cells into the scaffolds and the elimination of the waste). Doing the vacuum decreased this value until 22%. But it is clearly obvious that the gelation is the best way to reach our goal: the value is now close to zero. This could be explained by the same phenomenon of sedimentation of particles. At room temperature, there is more deposition of α-TCP than with the two other techniques, which means that less particles disrupt the gelatin matrix to create interconnectivity, and consequently there

will be more isolated pores.

The gelation process has an influence on the interconnectivity of pores. It could be explained by the fact that with gelation, there is no particles deposition at the bottom of the mould and so that, there are more particles incorporated to the gelatin matrix, which permit to reduce isolated porosity.

Incorporation of particles in the mixture increases the density of the scaffold. In figure 5.19, for a scaffold of gelatin 5 wt % and 1.5 wt % of α-TCP, done with three distinct experimental conditions (room temperature, vacuum and gelation) the closed porosity is varying a lot. Indeed, for the sample at room temperature (without any process applied), there is 33% of closed pores, which is not acceptable for the application of our scaffolds. This rate decreases with the application of the vacuum and decreases again until almost zero when gelation is applied.

The table, figure 5.18, presents contents of closed porosity in each type of scaffold.

% closed porosity	**Room temperature**	**Vacuum**	**Gelation**
Gelatin 5 wt %	No value	No value	6.4
gelatin5wt% +α-TCP 0.5wt%	33	21	0.5
gelatin5wt% +α-TCP 1.5wt%	43	22	0.5

Fig 5.18: table with closed porosity content at different experimental conditions

5.3.4 Compression test

A representative stress-strain curve for bone shows a linear elastic region, followed by a flat plastic region. It is necessary to mention that bone is a tough material at low strain rates but fractures more like a brittle material at high strain rates. Its increases while increasing mineral content. Figure 5.19 presents stress-strain curves of three different samples.

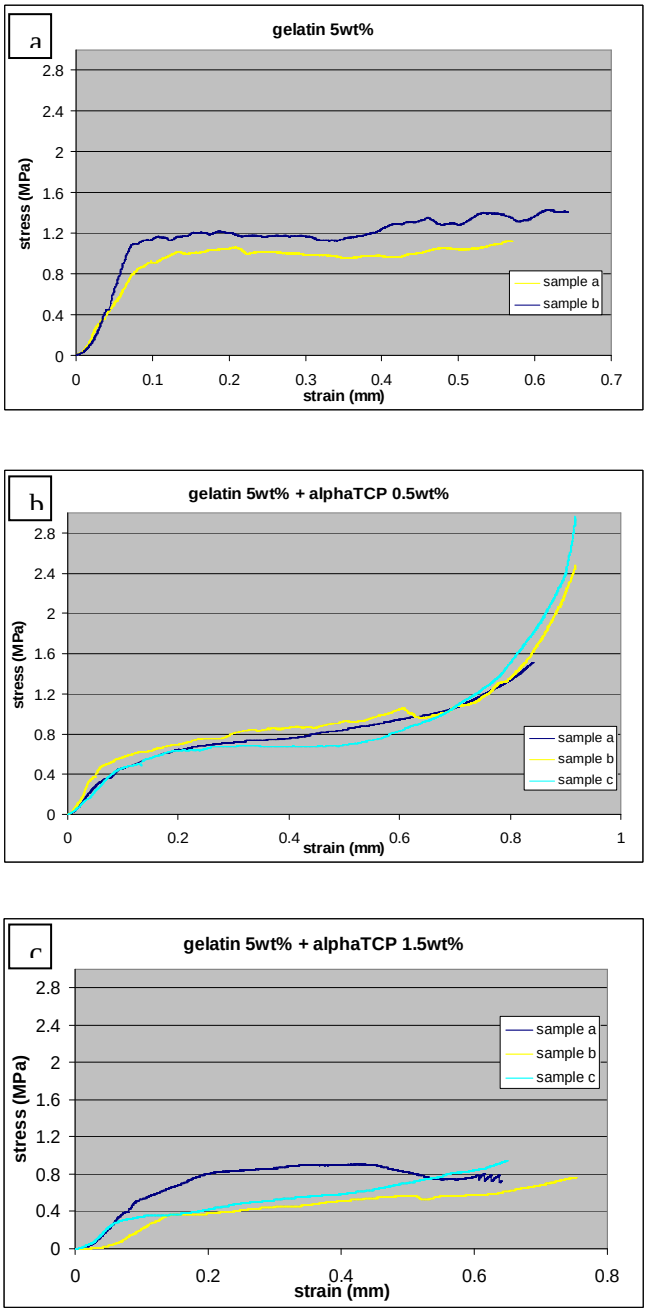

Fig 5.19: stress-strain curves of gelatin 5wt% (a), gelatin 5wt% with α-TCP 0.5wt% (b), and gelatin 5wt% with α-TCP 1.5wt% (c)

Figure 5.19.a reveals a linear elasticity at low stresses followed by a long collapse plateau, truncated by a regime of densification in which the stress rises steeply. (21) Young modulus, E, is the initial slope of the stress-strain curve. The young modulus is approximately 18,5MPa, and the stress is 1.2MPa for a strain equal to 0.5.

Figure 5.19.b, the difference in the mechanical behavior is obvious. The stress at 0.5 is now lower, 0.8MPa, so do the young modulus, 7MPa.

When the α-TCP content is increased until 1.5 wt %, in the figure 5.19.c, the young modulus is equal to 7.8MPa and the stress applied is 0.65MPa at 0.5 of strain.

At first, when we planned to add α-TCP to the scaffold, we thought that it will permit to increase their rigidity, and so that their young modulus, because adding mineral phase in a cement enhances its resistance. However, here, the results seem to be in contradiction with this affirmation. This phenomenon could be explained by the fact that adding α-TCP to gelatin also creates interconnected pores in the scaffold. These pores in the scaffold are responsible of the loss of rigidity.

5.4 Scaffolds with inorganic matrix

5.4.1 Morphology

The new perspective about this work is the creation of scaffolds with inorganic matrix, which have never been synthesized before. The matrix is constituted of α-TCP and gelatin is added as a binder. Several proportions of gelatin have been tried: 1%wt, 2 wt % and 5 wt %.

The objective in preparing those scaffolds is to generate mechanical interlocking of the crystals (figure 5.22) to improve the mechanical properties of the scaffold.

For each scaffold, 10 wt % of α-TCP was added. The scaffold with only 1 wt % of gelatin was very unstable and flexible: there was no cohesion between the particles. But, with 2 wt % and 5 wt % of gelatin, scaffolds were much better, with a good aspect and cohesion. The approach followed for the preparation of these scaffolds was very similar to the process of preparation of the organic ones, except for the mixing time, which was reduced to 1h, in order to maintain a high proportion of α-TCP. All samples were gelified before putting them in the freezer.

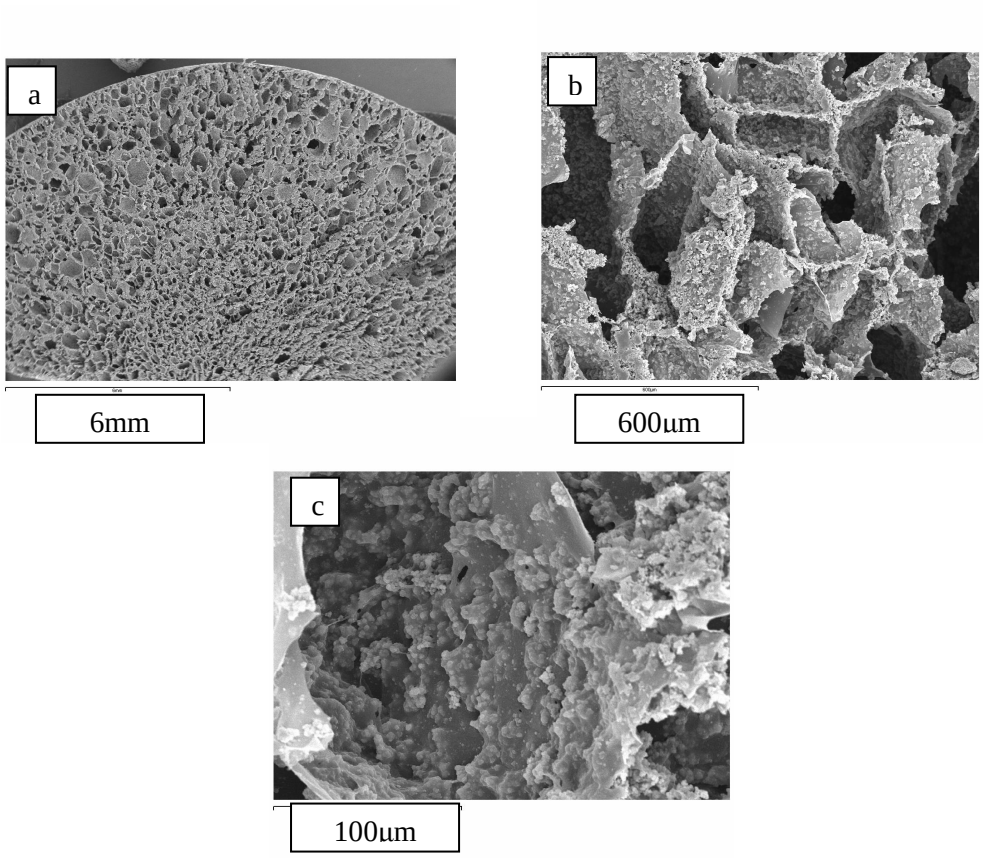

Fig 5.20 SEM images of scaffold with inorganic matrix (gelatin 5wt%+10wt% of α-TCP)

As clearly illustrated in these SEM pictures (figure 5.20), there is a porous interconnected network structure, which resembles the microstructure of the gelified samples. Much more particles of α-TCP are present in the matrix. The percentage of α-TCP is now 10 wt %, whereas it was 0.5 wt % and 1.5 wt % for the scaffolds with organic matrix.

5.4.2 Phase and structure

During the time of crosslinking, two reactions will occur. First of all, a reaction of cross linking of the gelatin, but also a reaction of hydrolysis of the α-TCP:

$$\underset{\alpha\text{-TCP}}{3\ \alpha\text{-}Ca_3(PO_4)_2} + H_2O \longrightarrow \underset{\text{CDHA}}{Ca_9(HPO_4)(PO_4)_5OH}$$

During the cross-linking, the immersion in water will permit to transform this α-TCP in calcium deficient hydroxyapatite, and then create interlocking between all those particles of α-TCP. If there are many particles of α-TCP and if they are closed sufficiently, bonds will be created and the scaffold will be strong enough.

So, in order to enhance this interlocking process, we have to minimize the fraction of HA created during the heating phase.

Figure 5.21 shows microstructure of a crosslinked sample made of 2wt% of gelatin.

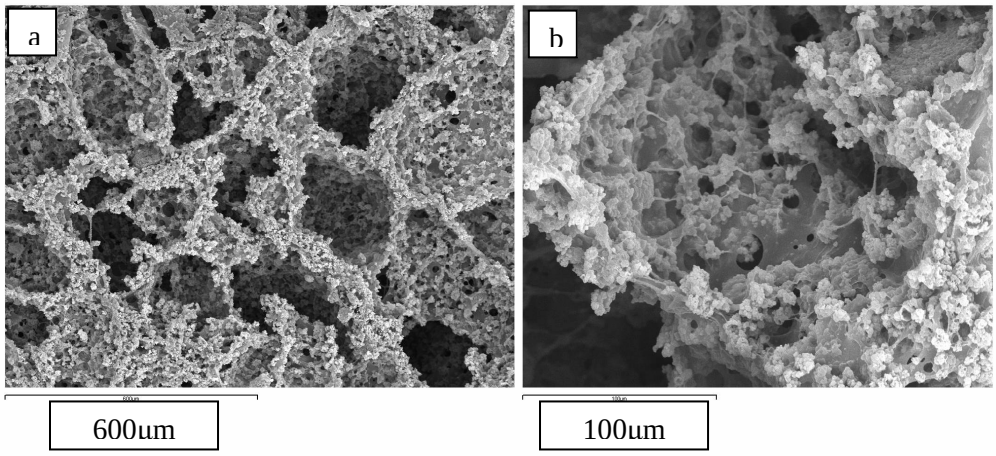

Fig 5.21: SEM pictures of an inorganic scaffold crosslinked with EDC-NHS

In the picture (a) of the figure 5.21, the particles of α-TCP composing the scaffold are clearly visible. They are all interlocked, thanks to cross linking. Indeed, the crosslinking allowed the hydrolysis of α-TCP in CDHA. Figure 5.22 explained this phenomenon of interlocking during hydrolysis.

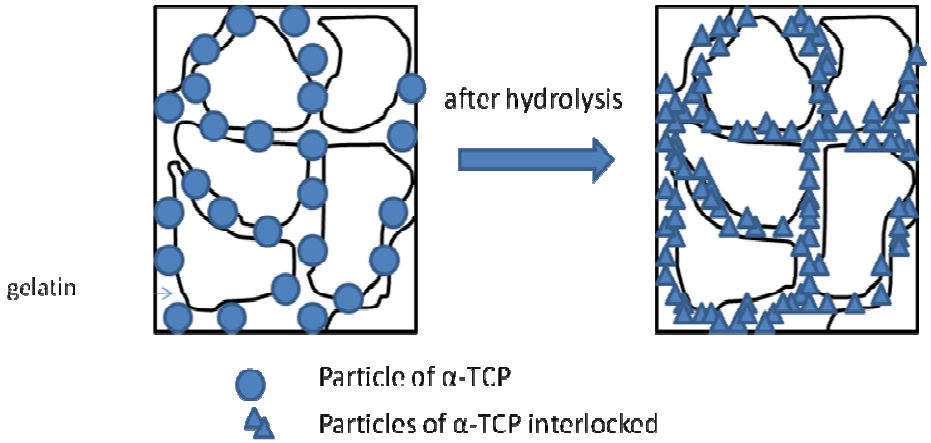

Fig 5.22: Hydrolysis of a sample made of gelatin 5wt% + α-TCP 10wt%

The XRD pattern (figure 5.23) shows the phases in presence in scaffolds non crosslinked and crosslinked.

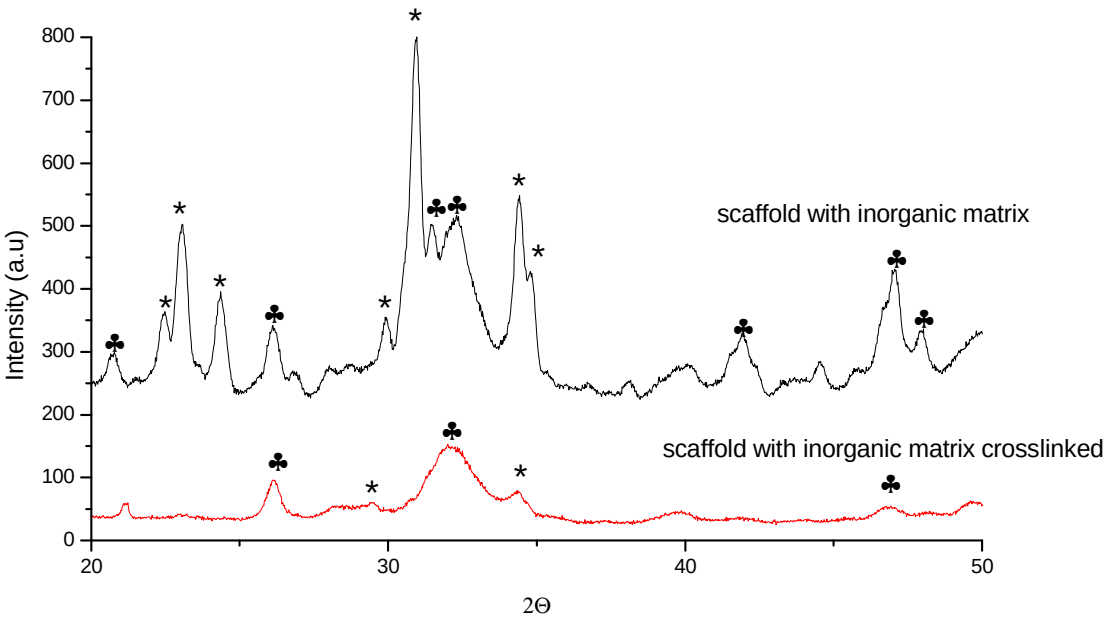

Fig 5.23: XRD pattern of scaffolds with inorganic matrix (gelatin 5 wt %+ α-TCP 10 wt %): influence of the crosslinking

There is a change in the chemical composition between a scaffold crosslinked and a scaffold not crosslinked. The crosslinking affects the structure of the gelatin but it also permits the hydrolysis of α-TCP in CDHA, which is demonstrates in this pattern. For the identification, the PDF-file number 09-0348 and 09-0432 were used to index α-TCP and HA respectively (see annex A-1).

5.4.3 Porosity

This graphic (figure 5.24) shows the effect of the amount of gelatin on the percentage of closed pores within two scaffolds (with gelatin 1wt% and gelatin 5wt%).

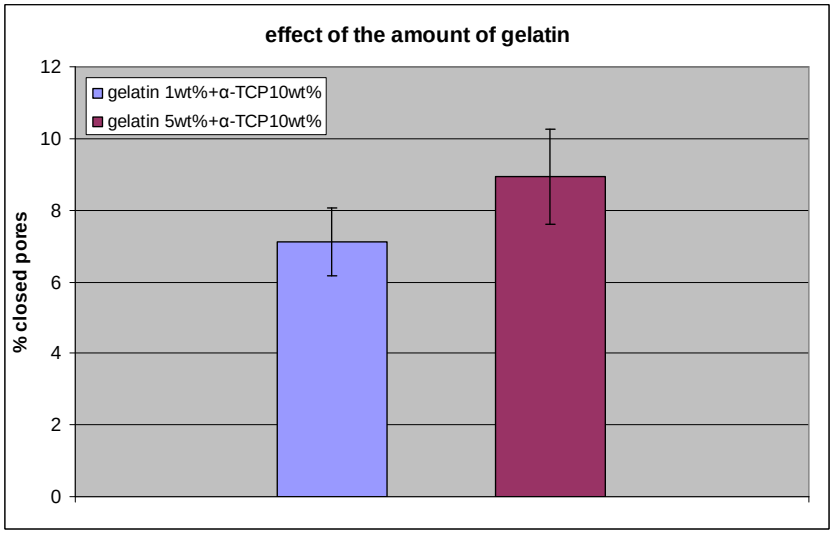

Fig 5.24: diagram demonstrating the effect of the gelatin amount

It demonstrates that the percentage of closed pores is situated between 7% and 9%. The amount of gelatin does not affect this proportion. These different proportions (1wt%, 2wt%, 5wt%) of gelatin were tested to see the effect of incorporation of α-TCP on this matrix. It also affects the cohesion of the scaffold.

5.4.4 Compression test

5.4.4.1 gelatin 5wt%

Curves from compression test are presented, figure 5.25.

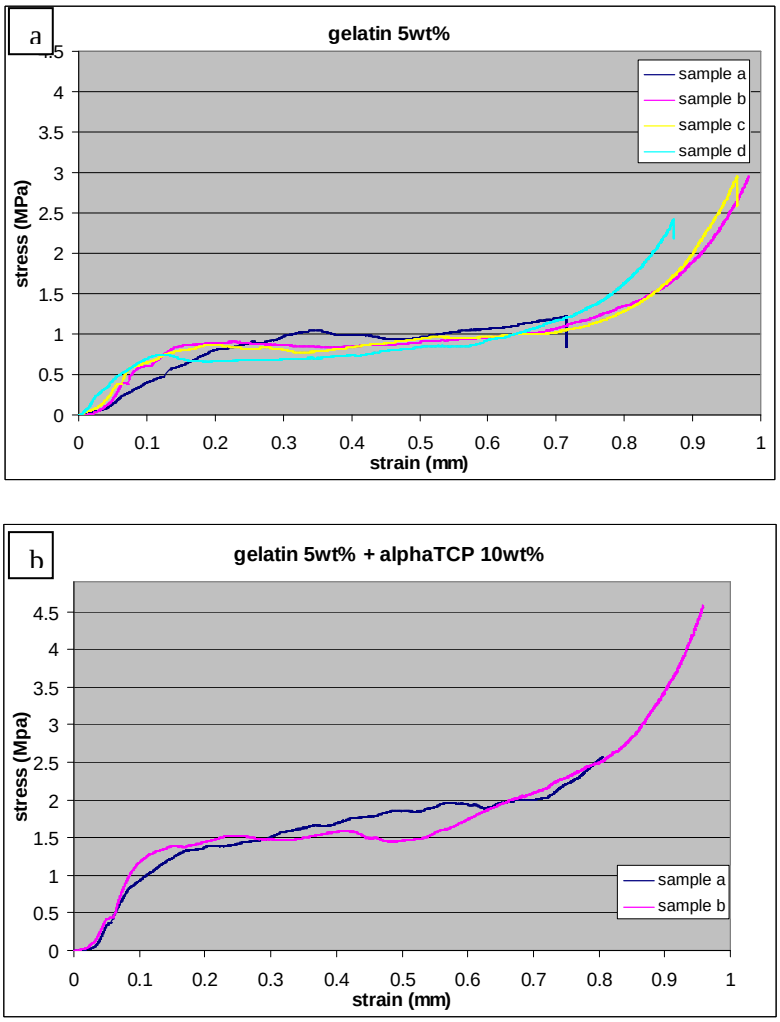

Fig 5.25: stress-strain curves of scaffolds made of gelatin 5wt% (a), gelatine 5wt% and α-TCP 10 wt % (b)

In the figure 5.25.a, this is the same type of gelatin scaffolds and we see the same stress of 1MPa at a strain of 0.5 and the same young modulus as curves on figure 5.19.a.

Adding particles of α-TCP make the scaffold more rigid. In figure 5.25.b, the young modulus is 5.5MPa and the stress at 0.5 is higher than for the scaffold without α-TCP (1.65MPa) (figure 5.25.a).

5.4.4.2 gelatin 2 wt %

The figure 5.26 is the result of a compression test made with samples containing only 2wt% of gelatin.

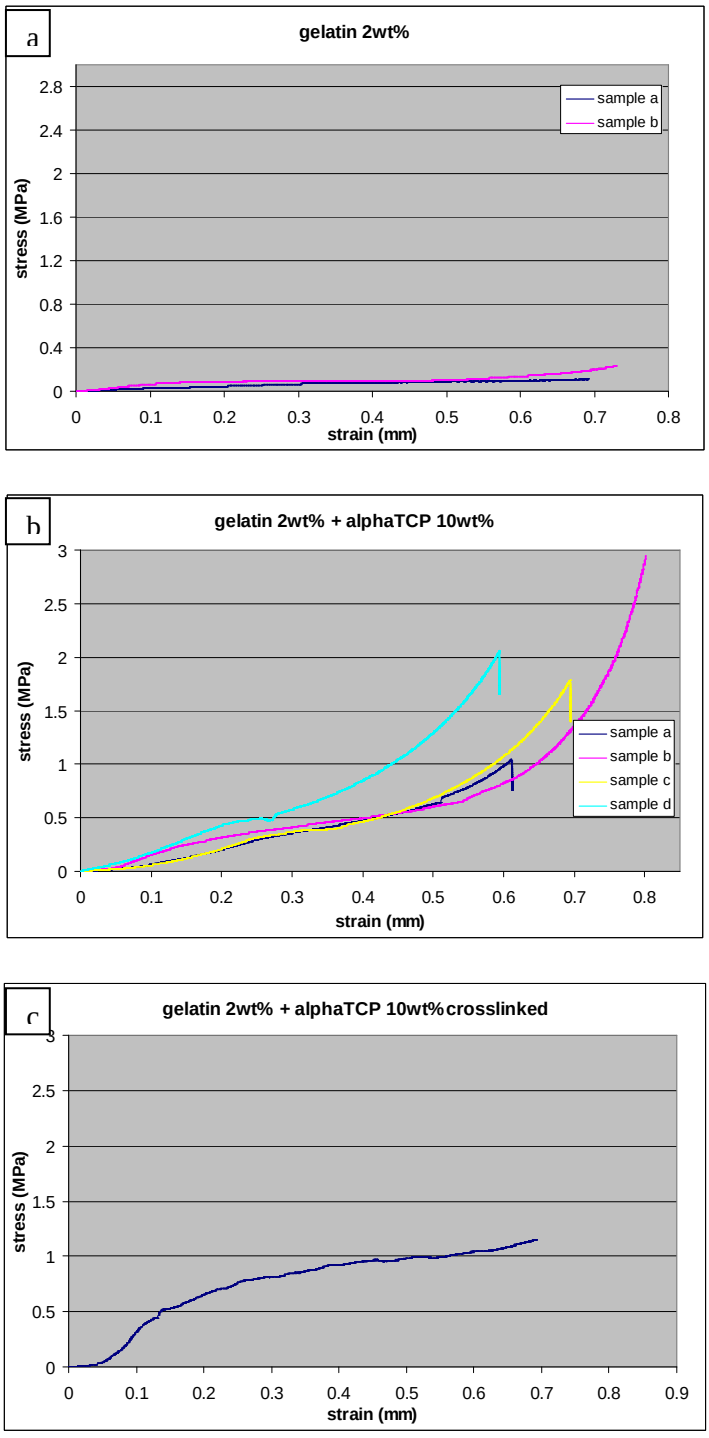

Fig 5.26: stress-strain curves of gelatin 2wt% (a), gelatine 2wt% and α-TCP 10wt% (b), gelatine 2wt% and α-TCP 10wt% crosslinked (c)

The scaffold of pure gelatin (figure 5.26.a) has a really small young modulus (0.17MPa) and a lower stress at strain equal to 0.5: 0.15MPa.

Adding 10wt% of TCP has an important effect of the mechanical resistance: the young modulus has been multiplied by 6. It is now equal to 1.14MPa. But the effect is more visible on the figure 5.26.b. The stress read for the same value of strain as before (0.5) has increased a lot: it is 0.8MPa (figure 5.26.b).

With cross-linking, the scaffold becomes more rigid and resistant under a compression load (figure 5.26.c). The stress is almost 1MPa and the young modulus is equal to 6.75MPa.

CONCLUSIONS

The objective of this project was to improve the existent process of fabrication of scaffolds with organic matrix, but especially the creation of scaffolds with inorganic matrix.

The first part of this work, the improvement of the existent process was successfully achieved: several parameters were examined. We have seen that letting the sample at room temperature before putting it in the freezer creates a damaged structure, with defects and a porosity non acceptable for our application.

Hence, the vacuum was studied. The structure network has been improved, and the rate of closed pores has decreased, which is a good point.
The last experimental condition tested, which gives the best result, was the gelation of the gelatin. With this technique, the percentage of closed pores is almost null and the porous microstructure is more homogeneous. Moreover, gelation, by avoiding particles sedimentation, increases the incorporation of α-TCP particles in the scaffold.

The crucial point of this project was the creation of scaffolds with inorganic scaffolds, which was the second part of the work. This creation was performed, giving really acceptable results, concerning the porosity, the amount of closed pores and also the mechanical resistance.

FUTURE PERSPECTIVES

This work is the very beginning in the field of scaffolds made of gelatin and α-TCP, especially for the one with inorganic matrix.

Crosslinking remains to improve. Indeed, the proportions used were appropriated but the final aspect of the scaffold, its porosity, or its mechanical resistance could be enhanced.

For scaffolds with inorganic matrix, proportions of reactives still need to be adjusted, in order to enhance the interlocking process and get the mechanical behaviour wanted.

Other techniques of characterization of porosity could be done, like mercury intrusion porosimetry.

ECONOMIC COSTS

In this part, a table (figure 0.1) with an estimation of the quantity of all the raw material used during the project is presente. The raw material includes all reactives which enter in the fabrication of the scaffolds of gelatin and calcium phosphate.

Producto	Quantity	Cuesto (€)
Calcium carbonate ($CaCOB_{3B}$)	96,8g	32,53
Calcium hydrogen phosphate ($CaHPOB_{4B}$)	263,2g	3,53
gelatin	255g	43.45
EDC	2.2mL	21.14
NHS	11.5g	10.81
Total		**111.46**

Fig 0.1: Cost of products used

The following table (figure 0.2) introduces an estimation of the costs of all techniques used during the work.

Técnica	**cost (€)/test or hour**	**Total technique cost (€)**
X rays diffraction	6,74	20,22
Compression test	3,02	24.16
Helium pycnometer	0.50	29.00
Microscopía SEM	31,5	189
Granulometry	19.93	59.79
Freeze dryer	2.84	340.8
IR	free	free
Total		**662.97**

Fig 0.2: Cost of techniques employed

ENVIRONMENTAL IMPACT

The project has been carried out, considering the potential impact on the environment.

The first material used was calcium phosphate. It is a natural material which does not have a negative impact on the environment. Moreover, the biomaterial department of the ETSEIB has a strict waste policy: all the cements wasted were thrown in a specific container.

The gelatin used was extracted from pig. It presents no danger for health and environment. It is a non toxic product.

The gloves and other plastic residues are also selectively stored.

ACKNOWLEDGEMENT

First of all, I would like to express my gratitude to Maria Pau Ginebra, for giving me the possibility to work in this laboratory. I discovered the specific field of biomaterials and I found my project really interesting.

I would like to thanks Montse for her support and assistance all along this project. This paper would not have been possible without your help. Thanks for your patience. ¡Moltes mercès per tot!

I would like to thanks also Román to introduce me all I had to know about cements and how to make them, for your support during these six months. Thank you for being so generous and helpful.

I am grateful to Txell also for teaching me about the equipment, and for many other things, thank you very much!

I want also to express my gratitude to Gemma, who dedicated me time for helping me when I was in need.

Thanks a lot to all personal of the laboratory of biomaterials of the ETSEIB, for all your help and the good conditions of working.

REFERENCIES

(1) J. Teot, Le tissu osseux, Coll. Biologie de l'appareil locomoteur, Broché, 1989

(2) http://www.webbooks.com/eLibrary/Medicine/Physiology/Skeletal/Skeletal.htm

(3) M. Zandi, H. Mirzadeh, C. Mayer, Early stages of gelation in gelatin solution detected by dynamic oscillating rheology and nuclear magnetic spectroscopy, European Polymer Journal, 1480–1486, 2007

(4) M. Bohner, U. Gbureck, J.E. Barralet, Technological issues for the development of more efficient calcium phosphate bone cements: A critical assessment, Biomaterials 26, 6423–6429, 2005

(5) E. Fernandez, F.J Gil, M.P. Ginebra, F.C.M. Driessens, J.A. Planell, Calcium phosphate bone cement for clinical applications, Part I: solution chemistry, Journal of Materials Science, 169-176, 1999

(6) E. Fernandez, F.J Gil, M.P. Ginebra, F.C.M. Driessens, J.A. Planell, Calcium phosphate bone cement for clinical applications, Part II: precipitate formation during setting reactions, Journal of Materials Science, 177-183, 1999

(7) A. Almirall, G. Larrecq, J.A. Delgado, S. Martinez, J.A. Planell, M.P. Ginebra, Fabrication of low temperature macroporous hydroxyapatite scaffolds by foaming and hydrolysis of an α-TCP paste, Biomaterials, 3671-3680, 2004

(8) D.L. Batchelara, M.T.M. Davidson, W. Dabrowski, I.A. Cunningham, Bone-composition imaging using coherent-scatter computed tomography: Assessing bone health beyond bone mineral density, Med. Phys. 33, 2003

(9) P. A. Webb, An Introduction to the physical characterization of materials by mercury intrusion porosimetry with emphasis on reduction and presentation of experimental data, Micromeritics Instrument Corp., 2001

(10) S.Deville, Freeze-Casting of Porous Ceramics: A Review of Current Achievements and Issues, Advanced engineering materials, 10, No. 3, 2008

(11) HW. Kim, J.C. Knowles, HE. Kim, Hydroxyapatite and gelatin composite foams processed via novel freeze-drying and crosslinking for use as temporary hard tissue scaffolds, Wiley InterScience, 2004

(12) http://www.beckmancoulter.com/coultercounter/product_LS13320.jsp

(13) Telstar brochure, Freeze dryer cryodos

(14) http://acept.asu.edu/PiN/rdg/elmicr/elmicr.shtml

(15) Micromeritics brochure, Helium pycnometry

(16) H.W Kim, J.C. Knowles, H.E Kim, Porous Scaffolds of Gelatin–Hydroxyapatite Nanocomposites Obtained by Biomimetic Approach: Characterization and Antibiotic Drug Release, Wiley InterScience, 2005

(17) A. Tamilsevan, D. Zhang, Cohesive energy calculation for cortical bone matrix, Bioengineering Conference, Proceedings of the IEEE 28th Annual Northeast, 2002

(18) J. Hashimi, L. Looney, M. S. J. Hashmi, The enhancement of wettability of SiC particles in cast aluminium matrix composites, Journal of Materials Processing Technology 119, 329-335, 2001

(19) K.B. Djagny, Z. Wang, S. Xu, Gelatin: A valuable protein for food and pharmaceutical industries: Review, Critical Reviews in Food Science and Nutrition, pg. 481, 2001

(20) F. Franks, N. Murase, Nucleation and crystallization in aqueous systems during drying: Theory and practice, Pure & Appl. Chem, Vol. 64, No. 11, 1992

(21) L. J. Gibson, M. F. Ashby, Cellular solids, structure and properties, second edition, Cambridge university press, 1997

Other referencies:

- J.Y Rho, R.B Ashman, C.H Turner, Young's modulus of trabecular and cortical bone material: ultrasonic and microtensile measurements, Biomech 26, 1993

- M.P. Ginebra, M.G. Boltong, E. Fernandez, J.A. Planell, F.C.M. Driessens, Effect of various additives and temperature on some properties of an apatitic calcium phosphate cement, Journal of Materials Science, 612-616, 1995

- J.R. Jones, G. Poologasundarampillai, R.C. Atwood, D. Bernard, P.D. Lee, Non-destructive quantitative 3D analysis for the optimisation of tissue scaffolds, Biomaterials, 1404-1413, 2007

- A.G. Mikos, J.S. Temenoff, Formation of highly porous biodegradable scaffolds for tissue engineering, Electronic Journal of Biotechnology, July 28, Vol.3 No.2, 2000

- S. Deville, E. Saiz, A.P. Tomsia, Ice-templated porous alumina structures, Acta Materialia, 1965-1974, 2007

- F.J. O'Brien, B.A. Harley, I.V. Yannas, L.Gibson, Influence of freezing rate on pore structure in freeze-dried collagen-GAG scaffolds, Biomaterials, 1077-1086, 2004

- C.T. Buckley, K.U. O'Kelly, Regular scaffold fabrication techniques for investigations in tissue engineering, Bio-Mechanical Engineering,147-166, 2004

- J.H. de Groot, A.J. Nijenhuis, P. Bruin, A.J. Pennings, R.P.H. Veth, J. Klompmaker and H.W.B. Jansen, Preparation of porous biodegradable polyurethanes for reconstruction of meniscal lesions, Colloid Polymer Science, 1073-1081, 1990

- G. Vargas, J.L. Acevedo, J. López, J. Romero, Study of cross-linking of gelatin by ethylene glycol diglycidyl ether, Materials Letters 62, 3656–3658, 2008

- S. Deville, E. Saiz, A.P. Tomsia, Freeze casting of hydroxyapatite scaffolds for bone tissue engineering, Biomaterials, 5480–5489, 2006

- J.D. Kretlow, A.G. Mikos, From Material to Tissue: Biomaterial Development, Scaffold Fabrication, and Tissue Engineering, Wiley InterScience, 2008

- W. Abdelwahed, G. Degobert, S. Stainmesse, H. Fessi, Freeze-drying of nanoparticles: Formulation, process and storage considerations, Advanced Drug Delivery Reviews 58, 1688–1713, 2006

- IUPAC J. Colloid Interface Chem.; Pure Appl. Chem., 31, 578, 1972

ANNEX

09-0432 Quality: I
CAS Number: 1306-06-5
Molecular Weight: 502.32
Volume[CD]: 528.80
Dx: 3.155 Dm: 3.080
Sys: Hexagonal
Lattice: Primitive
S.G.: P63/m (176)
Cell Parameters:
a 9.418 b c 6.884
α β γ
SS/FOM: F30=54(.0158, 35)
I/Icor:
Rad: CuKa1
Lambda: 1.54056
Filter:
d-sp: Guinier
Mineral Name:
Hydroxylapatite syn

Ca5 (P O4)3 (O H)
Calcium Phosphate Hydroxide
Ref: de Wolff, P., Technisch Physische Dienst, Delft, The Netherlands, ICDD Grant-in-Aid

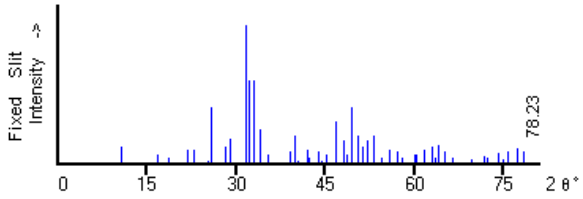

2θ	Int-f	h	k	l	2θ	Int-f	h	k	l	2θ	Int-f	h	k	l
10.820	12	1	0	0	43.804	8	1	1	3	63.443	4	5	1	0
16.841	6	1	0	1	44.369	2	4	0	0	64.078	13	3	0	4
18.785	4	1	1	0	45.305	6	2	0	3	64.078	13	3	2	3
21.819	10	2	0	0	46.711	30	2	2	2	65.031	9	5	1	1
22.902	10	1	1	1	48.103	16	3	1	2	66.386	4	4	2	2
25.354	2	2	0	1	48.623	6	3	2	0	66.386	4	4	1	3
25.879	40	0	0	2	49.468	40	2	1	3	69.699	3	5	1	2
28.126	12	1	0	2	50.493	20	3	2	1	71.651	5	4	3	1
28.966	18	2	1	0	51.283	12	4	1	0	71.651	5	4	0	4
31.773	100	2	1	1	52.100	16	4	0	2	72.286	4	5	2	0
32.196	60	1	1	2	53.143	20	0	0	4	72.286	4	2	0	5
32.902	60	3	0	0	54.440	4	1	0	4	73.995	7	4	2	3
34.048	25	2	0	2	55.879	10	3	2	2	75.022	3	3	2	4
35.480	6	3	0	1	57.128	8	3	1	3	75.022	3	6	0	2
39.204	8	2	1	2	58.073	4	5	0	1	75.583	9	2	1	5
39.818	20	3	1	0	59.938	6	4	2	0	76.154	1	4	3	2
40.452	2	2	2	1	60.457	6	3	3	1	77.175	11	5	1	3
42.029	10	3	1	1	61.660	10	2	1	4	78.227	9	5	2	2
42.318	4	3	0	2	63.011	12	5	0	2					

09-0348 Quality: *
CAS Number: 7758-87-4
Molecular Weight: 310.18
Volume[CD]: 2871.21
Dx: 2.870 Dm: 2.814
Sys: Orthorhombic
S.G.:
Cell Parameters:
a 15.22 b 20.71 c 9.109
α β γ
SS/FOM: F30=16(.0192, 95)
I/Icor:
Rad: CuKa1
Lambda: 1.5405
Filter:
d-sp: Guinier

α-Ca3 (P O4)2
Calcium Phosphate
Ref: de Wolff, P., Technisch Physische Dienst, Delft, The Netherlands, ICDD Grant-in-Aid

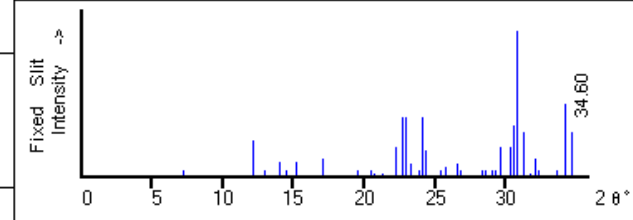

2θ	Int-f	h	k	l	2θ	Int-f	h	k	l	2θ	Int-f	h	k	l
7.181	4	1	1	0	25.801	6	0	6	0	34.602	30	0	8	0
12.097	25	1	1	1	26.585	8	3	1	2					
12.970	4	0	2	1	26.748	4	4	3	0					
14.068	10	1	3	0	28.307	4	2	6	0					
14.461	4	2	2	0	28.585	4	2	4	2					
15.184	10	2	0	1	29.061	4	4	4	0					
17.103	12	0	4	0	29.256	4	5	0	0					
19.493	4	0	0	2	29.653	20	5	1	0					
20.493	4	3	1	1	30.302	20	1	1	3					
20.735	2	2	4	0	30.600	35	4	0	2					
21.289	2	0	2	2	30.751	100	1	7	0					
22.205	20	1	5	0	31.247	30	5	1	1					
22.723	40	2	0	2	31.748	2	0	7	1					
22.901	40	2	4	1	32.099	12	5	3	0					
23.327	8	4	0	0	32.326	4	1	7	1					
23.835	4	3	3	1	32.727	<1	1	3	3					
24.097	40	1	3	2	32.900	<1	2	2	3					
24.298	18	1	5	1	33.599	4	5	3	1					
25.353	4	4	0	1	34.180	50	0	4	3